JOURNAL OF GEOPHYSICAL RESEARCH, VOL. 115, D04301, doi:10.1029/2009JD011880, 2010



# Production of lightning $NO_x$ and its vertical distribution calculated from three-dimensional cloud-scale chemical transport model simulations

Lesley E. Ott,[1] Kenneth E. Pickering,[2] Georgiy L. Stenchikov,[3,4] Dale J. Allen,[5] Alex J. DeCaria,[6] Brian Ridley,[7] Ruei-Fong Lin,[1] Stephen Lang,[8] and Wei-Kuo Tao[9]

Received 9 February 2009; revised 19 August 2009; accepted 15 October 2009; published 18 February 2010.

[1] A three-dimensional (3-D) cloud-scale chemical transport model that includes a parameterized source of lightning $NO_x$ on the basis of observed flash rates has been used to simulate six midlatitude and subtropical thunderstorms observed during four field projects. Production per intracloud ($P_{IC}$) and cloud-to-ground ($P_{CG}$) flash is estimated by assuming various values of $P_{IC}$ and $P_{CG}$ for each storm and determining which production scenario yields $NO_x$ mixing ratios that compare most favorably with in-cloud aircraft observations. We obtain a mean $P_{CG}$ value of 500 moles NO (7 kg N) per flash. The results of this analysis also suggest that on average, $P_{IC}$ may be nearly equal to $P_{CG}$, which is contrary to the common assumption that intracloud flashes are significantly less productive of NO than are cloud-to-ground flashes. This study also presents vertical profiles of the mass of lightning $NO_x$ after convection based on 3-D cloud-scale model simulations. The results suggest that following convection, a large percentage of lightning $NO_x$ remains in the middle and upper troposphere where it originated, while only a small percentage is found near the surface. The results of this work differ from profiles calculated from 2-D cloud-scale model simulations with a simpler lightning parameterization that were peaked near the surface and in the upper troposphere (referred to as a ''C-shaped'' profile). The new model results (a backward C-shaped profile) suggest that chemical transport models that assume a C-shaped vertical profile of lightning $NO_x$ mass may place too much mass near the surface and too little in the middle troposphere.

**Citation:** Ott, L. E., K. E. Pickering, G. L. Stenchikov, D. J. Allen, A. J. DeCaria, B. Ridley, R.-F. Lin, S. Lang, and W.-K. Tao (2010), Production of lightning $NO_x$ and its vertical distribution calculated from three-dimensional cloud-scale chemical transport model simulations, *J. Geophys. Res.*, *115*, D04301, doi:10.1029/2009JD011880.

## 1. Introduction

[2] The oxides of nitrogen, (NO + $NO_2$ = $NO_x$), are important $O_3$ precursors in the troposphere. Of the major sources of $NO_x$ in the troposphere, lightning remains the source with the greatest uncertainty and is particularly important because it produces $NO_x$ in the middle and upper troposphere where $NO_x$ is longer lived and can be more efficient at producing ozone than in the boundary layer. The representation of lightning $NO_x$ ($LNO_x$) in 3-D regional and global chemical transport models (CTMs) is critical to the models' representation of ozone and other species such as OH [e.g., *Stockwell et al.*, 1999, *Labrador et al.*, 2004]. *Labrador et al.* [2005] found that both the magnitude of the global $LNO_x$ source and its vertical distribution can substantially affect tropospheric trace gas concentrations in a global CTM. *Intergovernmental Panel on Climate Change* (*IPCC*) [2007] suggests a global $LNO_x$ source of 1.1–6.4 Tg N $yr^{-1}$ based on the work of *Boersma et al.* [2005]. However, *Schumann and Huntrieser* [2007] have comprehensively summarized estimates of global $LNO_x$ production and found the best estimate to be 5 ± 3 Tg N $yr^{-1}$.

[3] To adequately represent the $LNO_x$ source in global or regional models, the geographic distribution of flashes, average production of NO per flash, and vertical distribution of $LNO_x$ following convection must be specified. A variety

[1]Goddard Earth Science and Technology Center, University of Maryland, Baltimore County, Baltimore, Maryland, USA.
[2]Atmospheric Chemistry and Dynamics Branch, NASA Goddard Space Flight Center, Greenbelt, Maryland, USA.
[3]Department of Environmental Sciences, Rutgers University, New Brunswick, New Jersey, USA.
[4]Now at King Abdullah University of Science and Technology, Thuwal, Saudi Arabia.
[5]Department of Atmospheric and Oceanic Science, University of Maryland, College Park, Maryland, USA.
[6]Department of Earth Sciences, Millersville University, Millersville, Pennsylvania, USA.
[7]Atmospheric Chemistry Division, National Center for Atmospheric Research, Boulder, Colorado, USA.
[8]Science Systems and Applications, Inc., Greenbelt, Maryland, USA.
[9]Mesoscale Atmospheric Processes Branch, NASA Goddard Space Flight Center, Greenbelt, Maryland, USA.


0148-0227/10/2009JD011880$09.00

of schemes have been used to specify the horizontal distribution of flashes (e.g., using variables such as cloud top height, upward cloud mass flux, convective precipitation, and CAPE as predictors). *Allen and Pickering* [2002] have evaluated their use in global 3-D CTMs. The production of NO per flash has been examined using laboratory experiments, theoretical assumptions regarding the physics of lightning flashes, and observations obtained during field projects. Despite these efforts, a great deal of uncertainty remains regarding NO production on a per flash basis, as well as the relative production by intracloud (IC) and cloud-to-ground (CG) flashes. On the basis of previous studies, which suggested that IC flashes were less energetic than CG flashes (e.g., *Holmes et al.*, 1971), many studies of $LNO_x$ production have assumed that $P_{IC}$ is less than $P_{CG}$. *Price et al.* [1997] assumed that a CG flash produces approximately 1100 moles of NO and that an IC flash was one tenth as productive of NO as a CG flash in estimating global $LNO_x$ production.

[4] However, a number of more recent studies have suggested that $P_{IC}$ may be nearly as great as $P_{CG}$ or possibly greater than $P_{CG}$. *Gallardo and Cooray* [1996] suggested that IC flashes may dissipate nearly as much energy as CG flashes and therefore $P_{IC}$ may be on the order of $P_{CG}$. *Cooray* [1997] found that for the same amount of charge neutralized, IC flashes dissipated more energy than CG flashes. Supporting the hypothesis of *Gallardo and Cooray* [1996], a 2-D cloud-scale modeling study by *DeCaria et al.* [2000] suggested that the $P_{IC}/P_{CG}$ ratio is likely between 0.5 and 1.0 and a 3-D modeling analysis by *DeCaria et al.* [2005] narrowed this range between 0.75 and 1.0. A study by *Fehr et al.* [2004] used a 3-D cloud-scale model simulation of a storm observed over Germany, and by comparing with lightning and aircraft observations, concluded that on average, an IC flash produced 40% more NO than a CG flash. *X. Zhang et al.* [2003b] argued that IC flashes may dissipate 50–100% as much energy as CG flashes. *Rahman et al.* [2007] found that results from experiments with rocket-triggered lightning suggested that $NO_x$ production was associated with relatively long duration continuing currents, which may be greater in IC flashes than in CG flashes, leading to the implication that IC flashes may produce as much or possibly more $NO_x$ per flash than CG flashes. Recent estimates of energy dissipated by IC and CG flashes using electrical potential and charge density measurements by *Maggio et al.* [2009] also suggest IC flashes may dissipate as much or more energy than CG flashes. However, the laboratory measurements of *Wang et al.* [1998] showed a strong dependence of $LNO_x$ on pressure. Since a larger fraction of the flash channel of IC flashes is located at lower pressures than for a CG flash, the pressure dependence may offset the possible greater energy dissipation in IC flashes in terms of NO production.

[5] Uncertainty surrounds a number of other aspects of $LNO_x$ production in addition to the relative production of $NO_x$ by IC and CG flashes. *Chameides* [1986] demonstrated that the amount of NO produced in a lightning channel depended strongly on the temperature in the channel. In addition to a strong dependence on pressure, the laboratory experiments by *Wang et al.* [1998] showed that NO production per unit flash length is also strongly dependent on peak current. Estimates of $LNO_x$ production, either by unit energy, by flash length, or by flash, vary widely in the literature. A recent review article by *Schumann and Huntrieser* [2007] showed that estimates of production per flash energy or peak current range from 1.7 to $83 \times 10^{-7}$ moles NO $J^{-1}$ while estimates of production per unit flash length range from 1.7 to $22 \times 10^{-3}$ moles NO $m^{-1}$. Observations of production per flash varied over two orders of magnitude, though *Schumann and Huntrieser* [2007] recommend a mean value of 250 moles NO per flash with a range between 33 and 660 moles NO per flash.

[6] *Pickering et al.* [1998] presented vertical profiles of $LNO_x$ for use in 3-D CTMs based on the results of 2-D cloud-resolving model simulations of seven convective events. These simulations assumed the production scheme of *Price et al.* [1997]. $NO_x$ produced by CG flashes was distributed in the simulated storms from the surface to the $-15°C$ isotherm while $NO_x$ produced by IC flashes was distributed from the $-15°C$ isotherm to the cloud top. Average profiles of $LNO_x$ mass computed for the midlatitude continental, tropical continental, and tropical marine regimes showed peaks in mass near the surface and in the upper troposphere, leading many CTMs to adopt a C-shaped vertical distribution of $LNO_x$ mass.

[7] This paper has two primary objectives: (1) to summarize the results of 3-D cloud-resolved storm simulations yielding estimates of NO production per flash and (2) to update the vertical $LNO_x$ profile information of *Pickering et al.* [1998]. Six storms from field projects conducted in Germany, Colorado, south Florida, and Kansas/Oklahoma have been simulated using a 3-D cloud-scale chemical transport model (CSCTM) that includes a parameterized source of $LNO_x$. $LNO_x$ production per flash is estimated individually for five of the six storms. In this study, we present vertical distributions of $LNO_x$ calculated from each of these 3-D simulations as well as average vertical profiles for the midlatitude continental and subtropical events, which can be applied in regional and global CTMs. Section 2 describes the methodology used in these studies, while section 3 presents results from the individual storm simulations. Section 4 discusses the results of the storm case studies and their application to global models and remote sensing. Section 5 presents conclusions that may be drawn from this work.

## 2. Methodology

[8] Storms from the Cirrus Regional Study of Tropical Anvils and Cirrus Layers—Florida Area Cirrus Experiment [CRYSTAL-FACE; *Ridley et al.*, 2004; *Lopez et al.*, 2006], European Lightning Nitrogen Oxides Project [EULINOX; *Huntrieser et al.*, 2002], Stratosphere Troposphere Experiment: Radiation, Aerosols and Ozone [STERAO; *Dye et al.*, 2000], and Preliminary Regional Experiment for STORM [PRE-STORM; *Rutledge and MacGorman*, 1988] field projects were simulated. With the exception of the PRE-STORM event, all of these storms featured measurements of chemical and meteorological properties by research aircraft at anvil levels. The time, location, and peak current of CG lightning occurrences in all storms were recorded by ground-based systems, and during STERAO and EULINOX, total lightning activity (IC + CG) was mapped by a VHF interferometer. In addition, all experiments included exten-

sive satellite and radar observations of storm development and evolution.

[9] The dynamical evolution of each storm was simulated using a cloud-resolving model, and the temperature, wind, and hydrometeor fields were then used to drive the offline CSCTM. For each storm, various $LNO_x$ production per flash scenarios were simulated and model results were compared with in-cloud aircraft observations of $NO_x$. By comparing column mass and probability distribution functions (pdfs) of the observed and simulated storms, the most appropriate production scenario was estimated for each storm. At the end of the CSCTM simulation, the mass of N fixed by lightning was calculated at each model level, and the percentage of the total mass of $LNO_x$ was calculated for 1-km layers.

[10] A detailed description of the CSCTM is found by *DeCaria et al.* [2005]. The vertical resolution of the CSCTM is 0.5 km whereas the horizontal resolution is 2 km for all simulations, except the PRESTORM case which employed a 1.5 km horizontal resolution. At the resolutions used in this study, convection is explicitly resolved. The CSCTM uses a 15 s time step for calculation of advection and diffusion. Chemistry is updated every 30 s, and $LNO_x$ production calculated at 3 min intervals. In this version of the model, $LNO_x$ production is computed using observed IC and CG flash rates and a specified scenario of $P_{IC}$ and $P_{CG}$ to calculate the mass of NO injected into the cloud per time step. Both laboratory experiments [*Wang et al.*, 1998] and theoretical considerations [*Price et al.*, 1997] have pointed to a strong dependence of $LNO_x$ production on stroke peak current. Therefore, we have made initial estimates of $P_{CG}$ using these relationships because peak current data for return strokes are available from ground-based network observations of CG flashes. However, this assumption contributes to uncertainty in the results because recent work with rocket-triggered lightning [*Rahman et al.*, 2007] has suggested that return strokes are not the primary NO-producing phase of a lightning flash. Field experimental results from Tropical Convection, Cirrus and Nitrogen Oxides Experiment (TROCCINOX) in Brazil [*Huntrieser et al.*, 2008] have suggested a lesser dependence on stroke peak current.

[11] The NO produced by CG flashes is distributed unimodally in the vertical, while the NO produced by IC flashes is distributed bimodally based on the vertical distributions of very high frequency (VHF) sources of IC and CG flashes presented by *MacGorman and Rust* [1998]. The two modes correspond to the two main charge centers in a typical thunderstorm cloud. The vertical distributions of IC and CG lightning channels used in the model are shown in Figure 2 of *DeCaria et al.* [2005]. The modes of the IC distribution are nominally set at the heights of the $-15$ and $-45$°C isotherms. However, the vertical distribution of IC channels is modified as necessary in some storms by changing the upper mode isotherm to account for a higher or lower cloud top and to match the upper tropospheric peak in aircraft observations of $NO_x$. At each model level, the lightning NO is distributed uniformly to all grid cells within the 20 dBZ contour computed from simulated hydrometeor fields. For simulations of the 10 July STERAO and 21 July EULINOX storms, the CSCTM was modified to include a filamentary placement scheme discussed in section 3.2 and *Ott et al.* [2007]. A passive version of the CSCTM includes only the transport of tracer species and production of $LNO_x$. In this version, three types of $NO_x$ (pre-existing $NO_x$, CG $LNO_x$, and IC $LNO_x$) are transported without any chemical reactions and the results are used to estimate average $NO_x$ produced by IC and CG flashes. Various production scenarios are specified and the model results compared with in-cloud aircraft observations to determine a first estimate of the most appropriate $LNO_x$ production scenario for the storm in question.

[12] A version of the model that includes $O_3$ photochemistry is used to separate $NO_x$ into NO and $NO_2$ and obtain a final and best estimate of NO production by IC and CG flashes. The chemical mechanism for the STERAO storms is described by *DeCaria et al.* [2005]. In the CRYSTAL-FACE and EULINOX simulations, the chemical scheme is identical to that described by *DeCaria et al.* [2005] with the exception that in these cases, isoprene and propene chemistry were included. Initial profiles of ozone were constructed using out-of-cloud aircraft observations, and when necessary to fill gaps, climatological ozone profiles appropriate for the latitude of the storm in question. The CSCTM includes a simple scheme to represent the influence of clouds on photolysis rates based on the work of *Madronich* [1987] and fully described by *DeCaria et al.* [2005]. Clear-sky photolysis rates are calculated following *Stamnes et al.* [1988] using observed column ozone amounts measured by the Total Ozone Mapping Spectrometer (TOMS) or, in the case of the STERAO storms, ozonesondes launched from Boulder, Colorado. Perturbations to clear-sky photolysis rates are determined by cloud thickness with very thick clouds (deeper than 5 km) resulting in photolysis rates multiplied by a factor of 2 above the cloud and 0.1 below the cloud base with a linearly interpolated degree of enhancement at intermediate altitudes.

## 3. Results

### 3.1. Subtropical Events

[13] The CRYSTAL-FACE experiment was conducted over south Florida in July 2002, and two storms investigated during the campaign were simulated. The 29 July CRYSTAL-FACE storm was simulated using the NASA Goddard version of the nonhydrostatic PSU/NCAR (MM5) mesoscale model [*Tao et al.*, 2003b] with a horizontal resolution of 2 km and vertical resolution of 0.5 km. The MM5 simulation was initialized with fields from NCEP's Eta model. At 1700 UTC (1300 LT) on 29 July 2002, a powerful thunderstorm developed along the west coast of Florida near Fort Myers. While the storm intensified and moved north along the coast, the area in and above the anvil was sampled by the NASA WB-57 research aircraft from 1845 to 2011 UTC at altitudes ranging from 12.5 to 13.8 km. The coastal convection later merged with convection originating near Lake Okeechobee. Figure 1 shows the time series of CG flashes recorded by the National Lightning Detection Network (NLDN) from 1700 to 2300 UTC. The 29 July storm was an exceptionally strong lightning producer with 4168 CG flashes recorded during this period. Maximum CG flash rates exceed 30 flashes per minute. These lightning flash rates and their relationship to NO

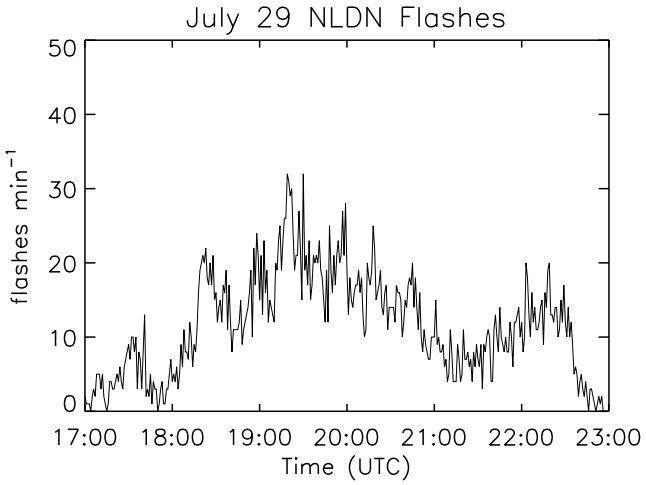


**Figure 1.** Time series of CG flash rates detected by the NLDN from 1700 to 2300 UTC (1300 to 1900 LT) for the 29 July CRYSTAL-FACE storm.

observations from the WB-57 aircraft have been discussed by *Ridley et al.* [2004].

[14] Simulated convection along the coast began earlier than observed by approximately 3 hours, but a number of storm features were successfully reproduced, including cloud top height and the direction of storm movement. The transport of CO (initial boundary layer maximum) and $O_3$ (initial stratospheric maximum) were calculated by the CSCTM using fields from the MM5 simulation of the 29 July storm and compared with in-cloud observations using pdfs. The model overestimated the frequency of values in the upper end of the frequency distributions for both CO and $O_3$ at anvil levels, suggesting that both upward and downward transport in the model may be too strong. However, the intense lightning activity in the thunderstorm and extremely elevated $NO_x$ mixing ratios (up to 10 ppbv) observed in the anvil indicate that the $LNO_x$ source in this storm was extremely strong. As a result, errors in transport are unlikely to significantly affect the estimate of $LNO_x$ production per flash in this case.

[15] Because the NLDN primarily recorded the occurrence of CG flashes during CRYSTAL-FACE, IC flash rates were estimated for the 29 July storm. NLDN flashes with positive peak current less than 10 kA are thought to be IC flashes [*Cummins et al.*, 1998]. These flashes were removed from the NLDN observations to estimate CG flash rates. The percentage of recorded flashes with positive peak current less than 10 kA was calculated during both the 29 July storm and the month of July as a whole. The percentage of such flashes in the 29 July storm was larger by a factor of 2.5 than the percentage for the month of July which may indicate an enhancement of the IC/CG ratio in the 29 July storm over the climatological value. To account for this enhancement, the south Florida climatological value for the IC/CG ratio of 2 from *Boccippio et al.* [2001] was multiplied by 2.5 to estimate an IC/CG ratio of 5. The upper mode of the vertical distribution of IC flash channel segments was set to −45°C.

[16] $P_{CG}$ was estimated to be approximately 590 moles NO on the basis of observed mean peak current (19 kA) and a relationship between peak current and energy dissipated from *Price et al.* [1997] which was modified by *DeCaria et al.* [2000] to account for the energy difference between positive and negative flashes. This relationship can be described by

$$E_{CG} = 1.823 \times 10^5 I_0, \quad (1)$$

where $I_0$ is peak current in A and $E_{CG}$ is energy in *J*. $E_{CG}$ is transformed to an estimate of $P_{CG}$ by multiplying by an assumed production of molecules NO per *J* of energy dissipated. In the work of *DeCaria et al.* [2000] and in this work, we assume $1 \times 10^{17}$ molecules of NO are produced per J of energy dissipated. Various values of the $P_{IC}/P_{CG}$ ratio were simulated, and the results compared with aircraft $NO_x$ observations (observed NO + estimated $NO_2$). $NO_2$ was estimated using NO and $O_3$ observations, and the photostationary state assumption because no direct measurements of $NO_2$ were available. Following the work of *Madronich* [1987], who demonstrated that actinic flux and photodissocation could increase within clouds, $NO_2$ mixing ratios were calculated assuming both clear-sky photolysis rates and rates enhanced by a factor of two. The observed column mass of N in $NO_x$ was calculated for the 1 km thick layer extending from 12.25 to 13.25 km by computing layer mean in-cloud $NO_x$ mixing ratios. Assuming that photolysis rates were enhanced in the cloud yielded a column mass of $6.6 \times 10^{-4}$ g N m$^{-2}$ while assuming that photolysis rates were unaltered by the cloud yielded a column mass of $7.0 \times 10^{-4}$ g N m$^{-2}$. Table 1 shows the sensitivity of CSCTM-calculated column mass to the assumed $P_{IC}/P_{CG}$ ratio. Assuming that an IC flash is on average 60% as productive of NO as a CG flash yields the most favorable comparison with column mass of nitrogen estimated from aircraft observations when an IC/CG ratio of 5 is assumed.

[17] Figure 2 shows the pdfs of observed and simulated in-cloud $NO_x$ assuming that $P_{IC}$ equals 50% and 60% of $P_{CG}$ and an IC/CG ratio of 5. When compared with observed pdfs at both 12.5 and 13 km, the production scenario that assumes a $P_{IC}/P_{CG}$ ratio of 0.5 compares more favorably than assuming a $P_{IC}/P_{CG}$ ratio of 0.6. Because the CSCTM $LNO_x$ placement scheme used in the CRYSTAL-FACE simulations is highly simplified (with all $LNO_x$ distributed within the 20 dBz contour according to the Gaussian vertical profiles), the model is not able to perfectly represent the variability reflected in in-cloud aircraft observations. To minimize these differences, observations and model results are compared using averages or pdfs. Still, differences between model output and observed $NO_x$ mixing ratios may result from the model's inability to fully represent the complexity of flash structures within the cloud. On the basis of comparison of simulated and

**Table 1.** Calculated Column Mass of N in $NO_x$ in the 29 July CRYSTAL-FACE Storm

| $P_{CG}$ (moles NO per flash) | $P_{IC}/P_{CG}$ (IC/CG = 5) | $P_{IC}/P_{CG}$ (IC/CG = 2) | Column Mass (g N m$^{-2}$) |
|---|---|---|---|
| 590 | 0.1 | 0.25 | $2.3 \times 10^{-4}$ |
| 590 | 0.5 | 1.3 | $6.0 \times 10^{-4}$ |
| 590 | 0.6 | 1.5 | $6.9 \times 10^{-4}$ |
| 590 | 0.75 | 1.9 | $8.3 \times 10^{-4}$ |
| 590 | 1.0 | 2.5 | $1.0 \times 10^{-3}$ |

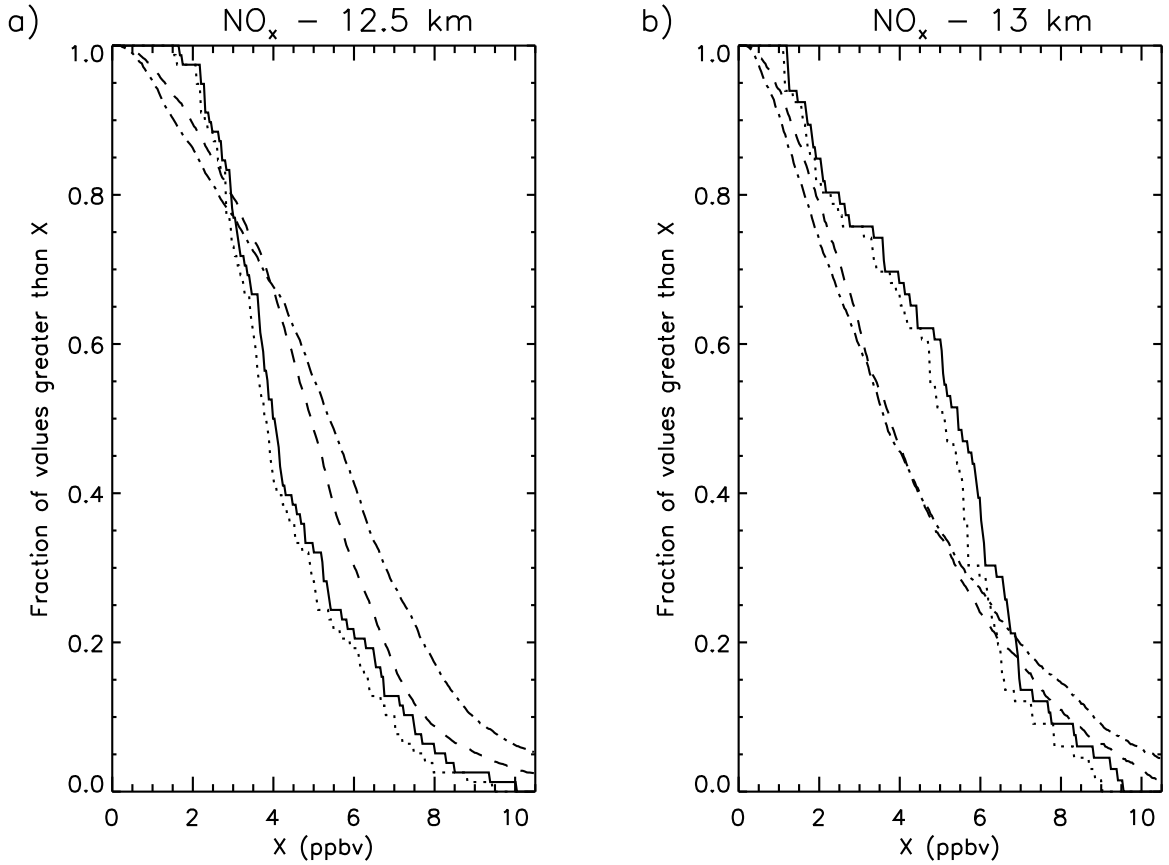


**Figure 2.** Pdfs of simulated and observed $NO_x$ at (a) 12.5 km and (b) 13 km for the July 29 CRYSTAL-FACE storm. Solid (dotted) line shows observed values assuming clear-sky (cloud enhanced) photolysis rates. Dashed (dot-dashed) line shows simulated values assuming $P_{IC}/P_{CG}$ of 0.5 (0.6).

observed pdfs and computed column mass, it is estimated that in the 29 July CRYSTAL-FACE storm an IC flash on average produced 50–60% as much NO as a CG flash while an average CG flash produced 590 moles NO. The assumption that an IC flash is one tenth as productive of NO as a CG flash significantly underestimated $NO_x$ when compared to column mass estimates calculated from in-cloud aircraft observations. When chemical reactions were simulated in addition to $LNO_x$ production and convective transport, a loss of $NO_x$ occurred because of conversion to reservoir species. The simulated column mass of N in $NO_x$ decreased by approximately 5% from the values shown in Table 1. The $P_{IC}/P_{CG}$ ratio of 0.6 was selected for the subsequent calculations because it continued to provide the best comparison with the column mass estimates derived from aircraft. The production scenario discussed above was deduced assuming that the IC/CG ratio in this particular storm was greater than the climatological IC/CG ratio for south Florida by a factor of 2.5. Because many more weak positive flashes (which are believed to be IC flashes) were recorded in this storm than was typical for the south Florida area during the month of July, it is likely that the IC/CG ratio was elevated above the climatological value. If instead the climatological IC-to-CG ratio of 2 is assumed, an IC flash must produce 50% more NO than a CG flash to match aircraft observations.

[18] It should be noted that the assumptions of IC/CG ratio, $P_{CG}$ value, and $P_{IC}/P_{CG}$ ratio contribute to uncertainty in the production scenario estimate. Figure 3 shows all the possible production scenarios that yield $NO_x$ mixing ratios which would match the observed column mass when IC/CG

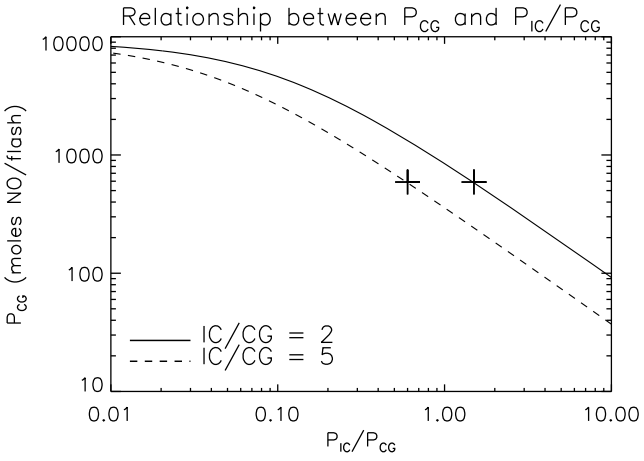


**Figure 3.** Relationship between $P_{CG}$ and the $P_{IC}/P_{CG}$ ratio necessary to match the column mass of N computed from aircraft observations. Solid (dashed) line shows the relationship when an IC/CG ratio of two (5) is assumed. Plus signs indicate the production scenarios when $P_{CG}$ is assumed to be 590 moles NO per flash on the basis of observed mean peak current.

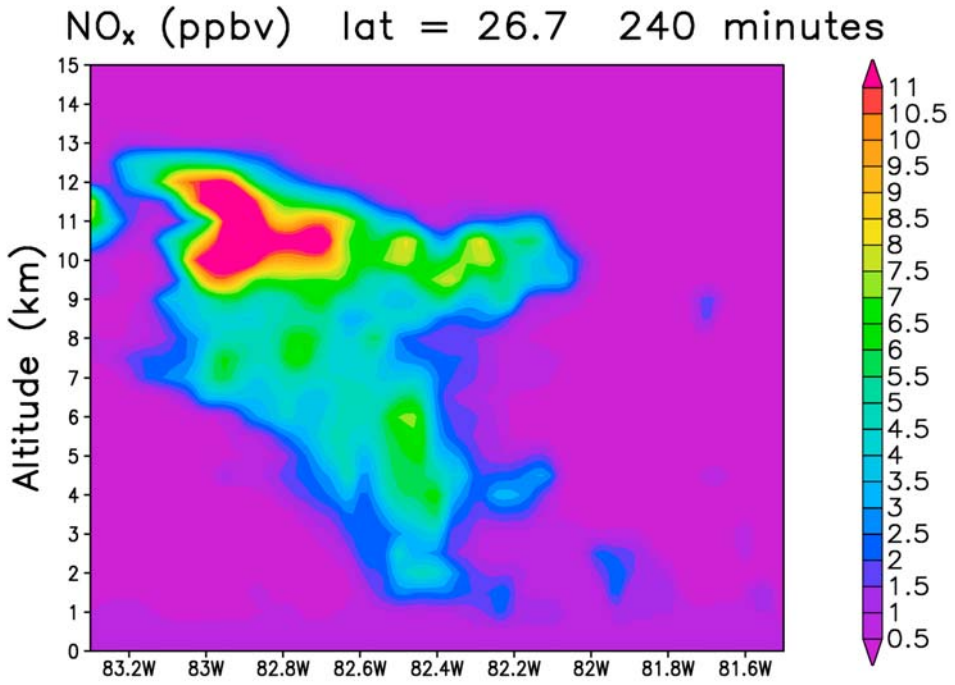


**Figure 4.** Vertical cross-section of simulated $NO_x$ in the July 29 CRYSTAL-FACE storm (assuming $P_{CG}$ = 590 moles NO, $P_{IC}$ = 354 moles NO, and an IC/CG ratio of 5) at 240 min.

ratios of two or five are assumed. The symbols on the curves show our best estimates ($P_{CG}$ = 590 moles/flash with $P_{IC}/P_{CG}$ at 0.6 and 1.5) based on the observed mean peak current. The majority of recent literature estimates of $P_{CG}$ range from 150 to 1100 moles NO per flash [e.g., *Schumann and Huntrieser*, 2007]. For this range of $P_{CG}$ values, the $P_{IC}/P_{CG}$ ratio could range from 0.3 to 6.1 in the 29 July CRYSTAL-FACE storm. If $P_{IC}$ is assumed to equal $P_{CG}$, then $P_{CG}$ must be between 350 and 850 moles NO per flash depending on the number of IC flashes which are assumed to have occurred. This analysis puts bounds on the uncertainty associated with assuming a single production scenario. If the IC/CG ratio was known to be 5 for this storm, the uncertainty would be reduced. $P_{IC}/P_{CG}$ would be in the 0.3–2.4 range (assuming $P_{CG}$ is between 150 and 1100 moles NO per flash). The assumption that IC and CG lightning are equally productive of NO on a per flash basis would yield a production of 350 moles NO per flash. This analysis demonstrates the need for observations of IC flashes in future experiments and more definitive information on the relationship between peak current or other electrophysical variables and $LNO_x$ production.

[19] A vertical cross section of simulated $NO_x$ through the core of the coastal storm at the end of the 240 min simulation is shown in Figure 4 (assuming $P_{CG}$ = 590 moles NO, $P_{IC}$ = 354 moles NO, and an IC/CG ratio of 5). Maximum $NO_x$ mixing ratios exceed 11 ppbv in the convective plume extending west from the Florida coast in the 10–12 km region. Figure 5 shows the vertical profile of the $LNO_x$ mass as it is introduced into the model domain, as well as its profile following convection from the same simulation as Figure 4. The bimodal distribution of the profile of injected $LNO_x$ mass reflects the bimodal distribution of IC flash channel segments calculated by the CSCTM. The upper mode peak is initially smaller in magnitude because the $LNO_x$ is distributed with a dependence on pressure as described by *DeCaria et al.* [2005]. Upward transport during the storm results in $LNO_x$ originally introduced into the model at altitudes near the lower mode peak residing near the top of the cloud following convection.

[20] On 16 July 2002, an isolated convective system developed northwest of Miami shortly after 1900 UTC (1500 LT) and was investigated as part of the CRYSTAL-FACE project. Over the next few hours, the storm moved

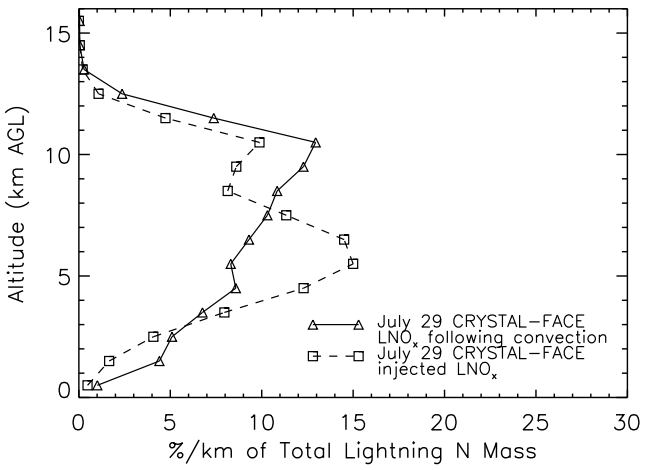


**Figure 5.** Vertical distributions of the percentage of $LNO_x$ mass per kilometer injected into the cloud and following convection for the 29 July CRYSTAL-FACE storm (assuming $P_{CG}$ = 590 moles NO, $P_{IC}$ = 354 moles NO, and an IC/CG ratio of 5).

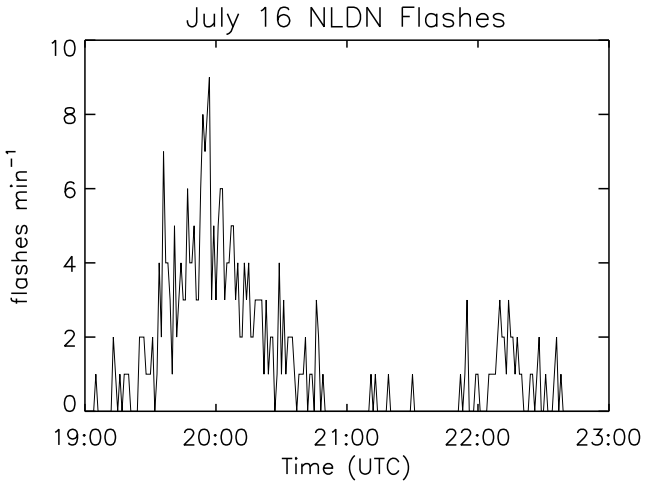


**Figure 6.** Time series of CG flash rates detected by the NLDN from 1900 to 2300 UTC (1500–1900 LT) for the 16 July CRYSTAL-FACE storm.

west across the Florida peninsula and was extensively sampled by the WB-57 from 1936 to 2306 UTC at altitudes ranging from 9 to 15.5 km AGL. The storm was simulated using the Advanced Regional Prediction System (ARPS) described by *Xue et al.* [2000, 2001] with a horizontal resolution of 2 km and vertical resolution varying from 25 m near the surface to 0.5 km near the top of the model domain at approximately 25 km. A number of different types of observations, including radar reflectivity, were assimilated into the simulation. The simulated temporal evolution of the storm matched observations well, as did storm size. The CSCTM was used to calculate the transport of tracer species CO and $O_3$ using fields from the ARPS simulation and a comparison of model results with anvil aircraft observations showed that the model adequately represented transport within the storm.

[21] Figure 6 shows the time series of flash rates recorded by the ground-based NLDN from 1900 to 2300 UTC. In contrast to the 29 July CRYSTAL-FACE storm, the 16 July storm was a relatively weak lightning producer with only 301 CG flashes recorded during this period and a maximum CG flash rate of 9 flashes per minute. The percentage of weak positive flashes (peak current <10 kA) was calculated during the 16 July storm and was over 20 times greater during the storm than for the month of July as a whole. Because the flash rate during the storm represented too small a sample to reliably make a large adjustment, IC flash rates were estimated from the observed CG flash rates and the climatological IC-to-CG ratio of two for south Florida from *Boccippio et al.* [2001]. On the basis of mean peak current of CG flashes recorded by the NLDN for this storm (23 kA), $P_{CG}$ was estimated to be 700 moles of NO. In this simulation, the upper mode of the IC flash channel distribution was set to −60°C because the tropopause was higher and the cloud top heights greater than in the 29 July CRYSTAL-FACE storm. Several different values of the $P_{IC}/P_{CG}$ ratio were simulated and the results compared with observations. The assumption that on average, an IC flash produces 75% as much NO as a CG flash yielded the most favorable comparison with the column mass of N in $NO_x$ estimated from observations when chemical reactions were not simulated. The simulation of chemistry led to a decrease in $NO_x$ mixing ratios because of conversion of $NO_x$ to reservoir species such as $HNO_3$ and PAN. In the storm core, where peak mixing ratios were ~5 ppbv when chemical reactions were not included, this decrease was approximately 1 ppbv. Chemical reactions resulted in decreases in $NO_x$ of approximately 0.5 ppbv in the anvil (where mixing ratios typically ranged from 1 to 2 ppbv before the simulation of chemical reactions). To match aircraft observations when chemical reactions were simulated, a $P_{IC}/P_{CG}$ ratio of 0.9 was needed. Figure 7 shows a vertical cross section of $NO_x$ calculated assuming this production scenario taken through the core of the storm after 180 min of simulation. Maximum $NO_x$ mixing ratios exceeding 5 ppbv are found at 6.5 km while lower concentrations are found in the upper part of the core and anvil.

[22] Figure 8 shows the percentage of the mass of N in $LNO_x$ in each kilometer-deep layer after both the 16 and 29 July CRYSTAL-FACE storms. Following the 29 July storm, the maximum in the vertical mass distribution is found at anvil levels (~10–11 km). In the case of the 16 July storm, the maximum is found in the 6–7 km layer, coincident with the lower mode of the vertical distributions of the $LNO_x$ source in the CSCTM. A smaller peak is found near the height of the upper mode of the distribution, at 12–13 km. These vertical $LNO_x$ mass distributions assume IC-to-CG ratios of two and five for the 16 and 29 July storms, respectively. Because IC-to-CG ratios may be highly variable and were estimated for these simulations, the results of a sensitivity test of the assumption of IC-to-CG ratios of two and five are shown for the 16 July storm in Figure 9a and for the 29 July storm in Figure 9b. For both storms, assuming an IC-to-CG ratio of two results in a slightly larger percentage of $LNO_x$ mass residing in the lower and middle portion of the cloud and a smaller percentage of $LNO_x$ mass near the cloud top (12–14 km for the 16 July and 10–12 km for the 29 July storm).

### 3.2. Midlatitude Continental Events

[23] The STERAO field project was conducted in June and July 1996 over northeastern Colorado to study $LNO_x$ production and convective transport of chemical species. CG lightning activity was monitored by the NLDN, while total lightning activity, including both CG and IC flashes, was mapped by a VHF interferometer. Two storms observed during the STERAO field project were simulated and $LNO_x$ production per flash was estimated in each. A similar analysis was conducted for one storm from the EULINOX field project conducted in southern Germany in July 1998. The fourth midlatitude storm simulated was from the 1985 PRESTORM experiment conducted over Kansas/Oklahoma.

[24] All four midlatitude storms were simulated using the 3-D Goddard Cumulus Ensemble (GCE) model, which is described by *Tao and Simpson* [1993] and *Tao et al.* [2003a]. The 12 July STERAO storm simulation was initialized with fields from the NCEP Eta model while the other three midlatitude cases were initialized with a single sounding. A description of the GCE simulation of the 12 July STERAO storm is contained in the work of *Stenchikov et al.* [2005], while the results of the chemical transport model simulation using the GCE temperature, wind and

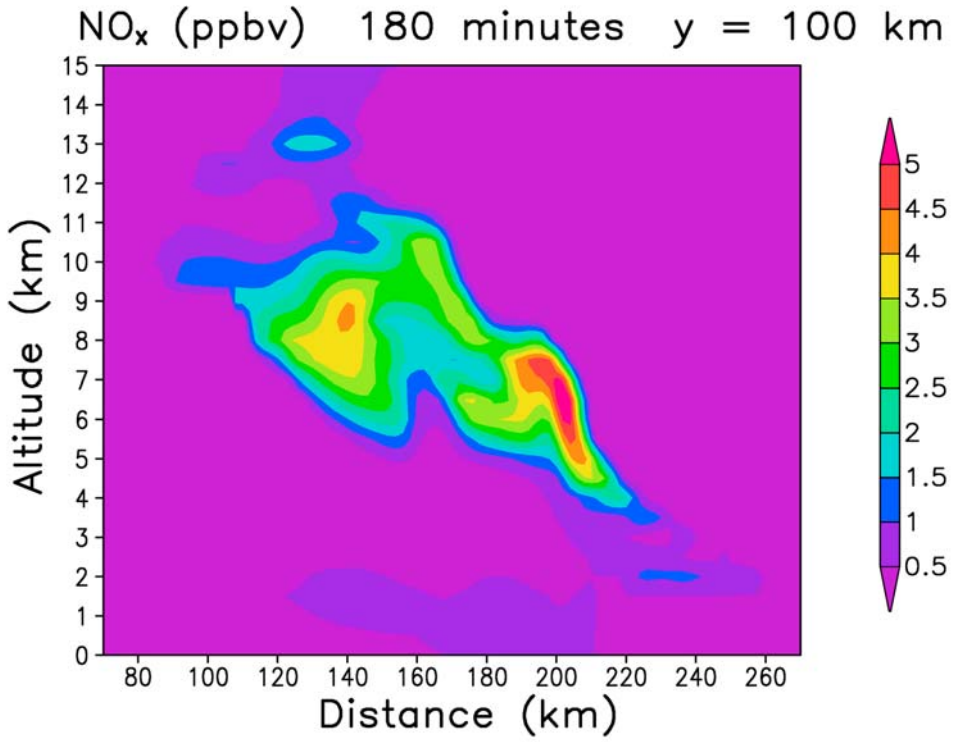


**Figure 7.** Vertical cross section of simulated $NO_x$ through the core of the 16 July CRYSTAL-FACE storm assuming $P_{CG}$ = 700 moles NO and $P_{IC}$ = 630 moles NO at 180 min.

hydrometeor fields are found by *DeCaria et al.* [2005]. Between 2000 and 2400 UTC (1400 and 1800 LT), 188 CG flashes and 2121 IC flashes were recorded by the NLDN and interferometer, respectively. Flash counts for the STERAO storms only include interferometer flashes with duration greater than 100 ms. Whether or not short duration flashes, which would not be recorded by some lightning detection systems, produce NO is an open question. *DeCaria et al.* [2005] estimated that $P_{CG}$ was 460 moles NO on the basis of the mean peak current of 15 kA. Assuming that an IC flash was equally as efficient at producing NO as a CG flash yielded the best comparison with observations in terms of mean vertical profile shapes while a $P_{IC}/P_{CG}$ ratio between 0.75 and 1 compared most favorably with observed column mass.

[25] On 10 July 1996, a multicellular thunderstorm organized in a northwest to southeast line developed near the Wyoming-Nebraska border at approximately 2100 UTC (1500 LT) and was observed as part of the STERAO campaign [*Dye et al.*, 2000; *Skamarock et al.*, 2000, 2003]. Research aircraft investigated the storm from 2237 to 0105 UTC. After 0115 UTC, the storm became unicellular with supercell chracteristics. IC lightning activity dominated throughout the lifetime of the storm with only 77 CG flashes and 3223 IC flashes recorded between 2201 and 0206 UTC. The University of North Dakota citation aircraft observed maximum NO mixing ratios of 1 ppbv approximately 60 km downstream of the storm cores [*Dye et al.*, 2000].

[26] The GCE model with a horizontal resolution of 2 and 0.5 km vertical resolution was used to simulate the 10 July STERAO storm and GCE temperature, wind and hydrometeor fields were used to drive the CSCTM. The GCE and CSCTM simulations were included in a cloud-chemistry model intercomparison study described by *Barth et al.* [2007]. Both the magnitude and height of the simulated peak updraft velocity compared well with observations. Convective transport was evaluated by comparing simulated CO and $O_3$ mixing ratios with observations obtained during two across-anvil transects. While the simulation underrepresented transport during the first transect, mixing ratios in the later transect were reproduced well by the CSCTM

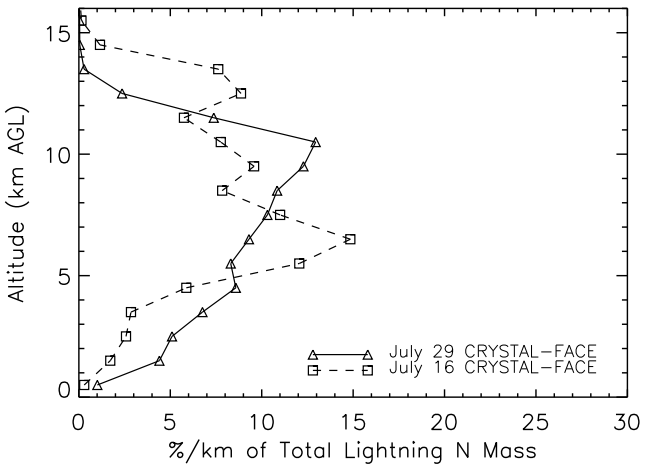


**Figure 8.** Vertical distributions of percentage of $LNO_x$ mass per kilometer following convection for two simulated subtropical storms.

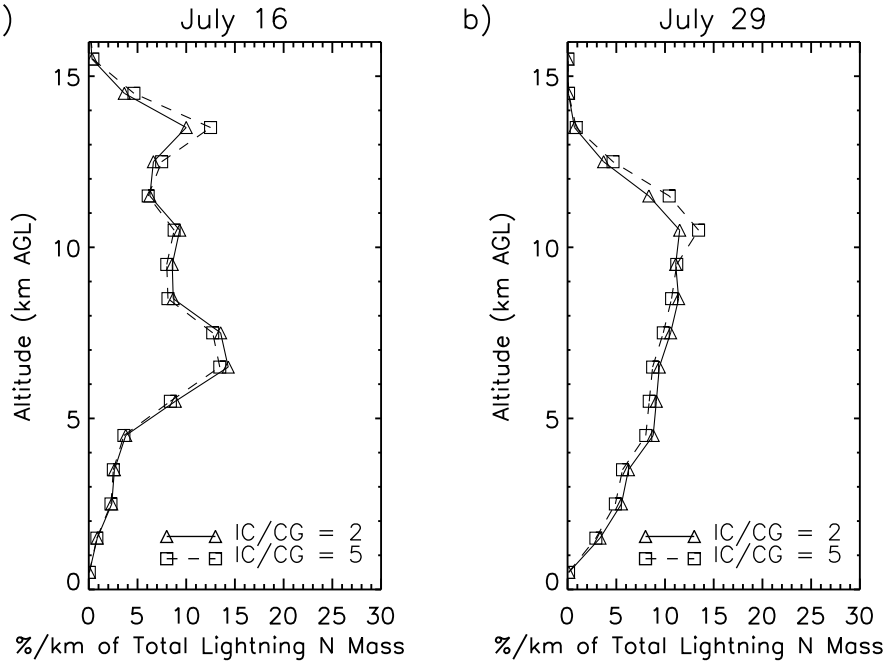


**Figure 9.** Vertical distributions of the percentage of $LNO_x$ mass per kilometer following convection for (a) the 16 July and (b) the 29 July CRYSTAL-FACE simulations assuming IC-to-CG ratios of two and five.

simulation, indicating that convective transport was adequate after an initial spin-up period.

[27] Simulated storm speed and cloud top heights compared favorably with radar observations. For the simulations of the 10 July STERAO and 21 July EULINOX storms, the parameterization of $LNO_x$ production was modified to simulate individual flashes. The method is fully illustrated by *Ott et al.* [2007]. Each flash is simulated by selecting grid cells at random from an area of the domain centered just downwind of the maximum updraft, which is similar in size to the area where lightning flashes typically occurred. The downwind location was chosen because plots of radar reflectivity and flash location by *Höller et al.* [2000] and *Dye et al.* [2000] show the majority of lightning activity occurring slightly downwind of the core updraft region. The number of grid cells included in a flash at each level is determined by vertical distributions adapted from the Gaussian distributions calculated in the original bulk method of $LNO_x$ parameterization described by *DeCaria et al.* [2005]. Simulations of both the 10 July STERAO and 21 July EULINOX storms using both the original and modified $LNO_x$ parameterizations show that the difference in parameterization produces little change in the vertical distribution of $LNO_x$ following convection. The upper mode of the IC flash channel distribution was set to $-50°C$ for the 10 July STERAO storm.

[28] In the 10 July STERAO storm, $P_{CG}$ was estimated to be approximately 390 moles on the basis of the observed peak current (13 kA) of CG flashes. Assuming a $P_{IC}/P_{CG}$ ratio of 0.5 matched in-cloud aircraft observations well when chemical reactions were not considered. When chemical reactions were simulated, the $P_{IC}/P_{CG}$ ratio was increased to 0.6 to match observations. Figure 10 shows a vertical cross section of calculated $NO_x$ through the core of the southernmost cell in the line of thunderstorms at the end of the 180 min simulation. $NO_x$ mixing ratios exceed 2.8 ppbv at 3.5 km above the surface but are only ~1 ppbv in the anvil region.

[29] The cloud-scale model intercomparison detailed by *Barth et al.* [2007] included a number of models which represented $LNO_x$ production through either parameterization or explicit simulation of the electrical environment within the 10 July cloud system. Estimates of lightning production used by different models ranged from 36 to 465 moles NO per IC flash and 36 to 1113 moles NO per CG flash. Despite the large range of values assumed, most of the models which included a lightning NO source compared reasonably with aircraft observations. Two models which predicted flashes using explicit cloud electrification schemes produced relatively small amounts of NO per flash (36–97 moles NO per flash). Our estimate of 390 moles NO per CG flash and a $P_{IC}/P_{CG}$ ratio of 0.6 yields an average production per flash of 240 moles NO per flash for this storm because lightning activity was dominated by IC flashes. This estimate is considerably larger than those provided by the two explicit models.

[30] *Barthe and Barth* [2008] introduced a new parameterization of $LNO_x$ which was tested on the 10 July STERAO storm. Vertical velocity was used to determine which convective cells were capable of producing lightning while flash rate was determined by ice mass flux. Placement of $LNO_x$ was filamentary, following *Ott et al.* [2007]. Using this scheme, *Barthe and Barth* [2008] estimated 121 ± 41 moles NO per flash. *Barthe and Barth* [2008] also performed a number of sensitivity simulations to identify which factors exerted the greatest influence on $LNO_x$ production in the 10 July STERAO storm. Their results suggest that placing $NO_x$ within a large volume of the cloud

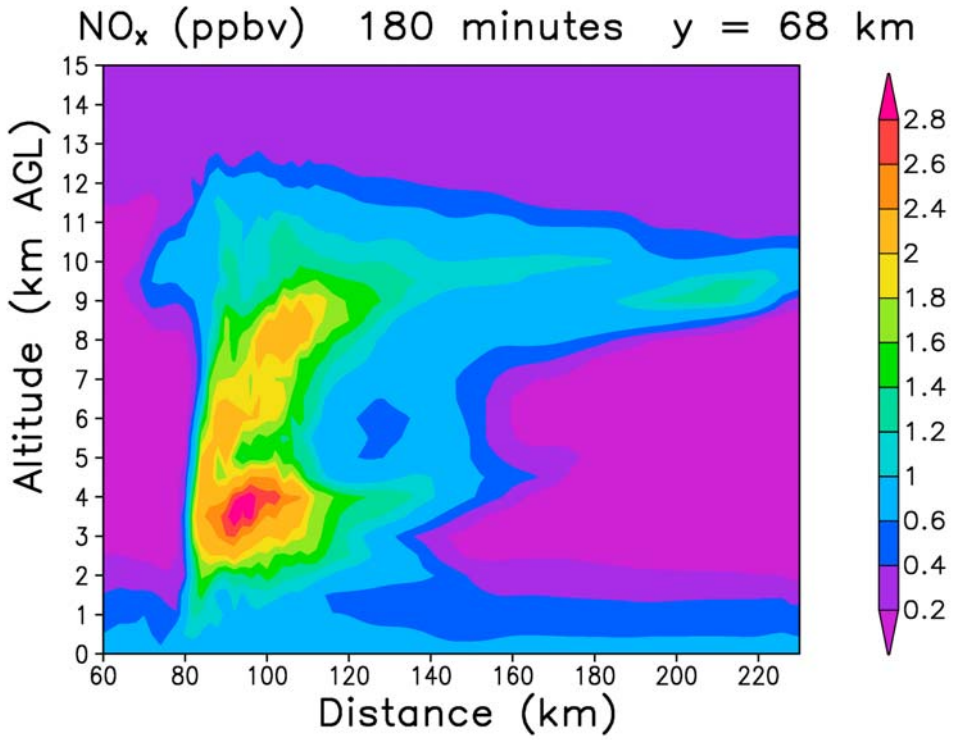


**Figure 10.** Vertical cross section of simulated $NO_x$ through the core of the southern cell of the 10 July STERAO storm assuming $P_{CG}$ = 390 moles NO and $P_{IC}$ = 234 moles NO at 180 min.

(i.e., within the 20 dBz contour) resulted in larger NO mixing ratios in the storm anvil than when a filamentary placement approach was used which may help explain the differences between estimated production per flash obtained by various models. While this may contribute to these differences, the simulations of the 10 July STERAO and EULINOX storms presented here both used the filamentary placement procedure described by *Ott et al.* [2007] and both estimated $LNO_x$ production in the same range as other simulations which distribute $LNO_x$ using a bulk approach (e.g., the 12 July STERAO storm, and the 16 and 29 July CRYSTAL-FACE storms). While the simulation of the storm electrical environment and the horizontal placement of $LNO_x$ within the cloud may impact the magnitude of the production estimate, other factors such as the manner of comparison of model results to observations may also play a role.

[31] The EULINOX field project was conducted in central Europe in June and July 1998 to study $LNO_x$ production over Europe. In addition to two research aircraft, the project included observations of CG lightning activity from the ground-based lightning detection system known as Blitz Informationsdienst von Siemens (BLIDS). One storm from the EULINOX project, which occurred on 21 July 1998 over southern Germany, was simulated using the GCE model. The storm developed as a single cell and after an initial period of intensification split into two distinct cells. The northernmost cell became multicellular in structure and was observed to decay rapidly, while the southern cell strengthened and developed supercell characteristics. The southern cell produced 360 CG and 2565 IC flashes between 1640 and 1900 UTC (1840 and 2100 LT), while the northern storm produced 289 CG and 815 IC flashes. The GCE simulation succeeded in reproducing a number observed storm features, including the cell-splitting. A full description of the GCE and CSCTM simulations is provided by *Ott et al.* [2007]. On the basis of the mean peak current (12 kA) of CG flashes, $P_{CG}$ was estimated to be 360 moles NO. The upper mode of the IC flash channel distribution was set to −45°C in this simulation. Several different values of $P_{IC}$ were simulated, and the scenario in which $P_{IC}$ is equal to $P_{CG}$ was found to compare most favorably with observations, though observed column mass was underestimated by 10%. To match observed column mass, the $P_{IC}/P_{CG}$ ratio needed to be increased to 1.15.

[32] In addition to the STERAO and EULINOX storms, the 10–11 June squall line observed during the PRESTORM project was simulated using the GCE model. The 10–11 June squall line has been documented extensively [e.g., *Johnson and Hamilton*, 1988; *Rutledge et al.*, 1988] and has previously been simulated using the 2-D version of the GCE [*Tao and Simpson*, 1993]. In this case, the horizontal resolution of the 3-D GCE was 1.5 km and vertical resolution varied from approximately 0.25 km near the surface to slightly more than 1 km near the top of the domain at 21.4 km. The GCE wind, temperature, and hydrometeor fields were interpolated to 0.5 km vertical resolution and used to drive the CSCTM simulation of the storm. During PRESTORM, the occurrence of CG lightning flashes was recorded by the National Severe Storms Laboratory's Lightning Location Network. On the basis of a time series of positive and negative CG flash rates from *Nielsen et al.* [1994], approximately 6500 CG flashes occurred during the storm's lifetime. Observations of total lightning

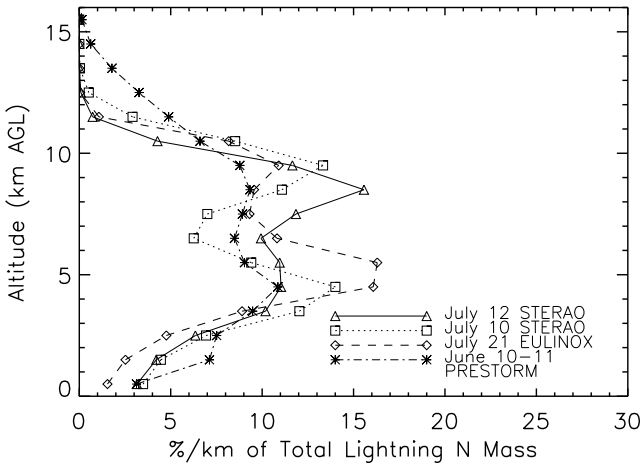


**Figure 11.** Vertical distributions of percentage of $LNO_x$ mass per kilometer following convection for four simulated midlatitude continental storms.

activity were unavailable, so the climatological IC/CG ratio of three for the region [*Boccippio et al.*, 2001] was assumed to estimate IC flash rates. The upper mode of the IC flash channel distribution was set to −45°C. No observations of the chemical environment of the squall line anvil are available. Therefore, it was not possible to estimate a production scenario for IC and CG flashes as in the other five storms. Instead, the average value of $P_{CG}$ calculated over the five other storms (∼500 moles NO per flash) was used along with an estimate of $P_{IC}$ that was 85% of $P_{CG}$ or 425 moles of NO.

[33] Figure 11 shows the vertical distribution of the mass of N in $LNO_x$ for the four midlatitude continental storms. The distributions for the four storms all reflect the double peaked distribution of $LNO_x$ produced by IC flashes in the model. There is variation between the simulations in the dominant mode of the lightning distributions. In the EULINOX and PRESTORM storms whose IC-to-CG ratios were on average 5 and 3, respectively, a higher percentage of $LNO_x$ mass is found near the height of the lower mode of the IC distribution, which is also the mode of the CG distribution. In the 10 July and 12 July STERAO storms, which had average IC-to-CG ratios of 33 and 8 during the time periods simulated, a greater percentage of $LNO_x$ mass resides near the height of the upper mode of the IC vertical distribution following convection. In addition to the IC-to-CG ratio, the dominance of the modes is likely affected by storm dynamics and the timing of IC and CG flashes in relation to the evolution of the storm.

## 4. Applications for Large-Scale Models and Remote Sensing

### 4.1. Vertical Distribution of Lightning $NO_x$ Mass

[34] We have presented results from the simulations of six thunderstorms using the 3-D CSCTM. Figure 12a shows the average vertical distribution of the mass of N in $LNO_x$ calculated by averaging the case studies in the subtropical regime, and Figure 12b shows the average vertical distribution for storms in the midlatitude regime overlaid with the vertical distribution calculated by *Pickering et al.* [1998]. Both plots are overlaid with smooth curves fit to the regime average. Table 2 lists the percentages of $LNO_x$ mass in each 1-km layer taken from the smoothed curves. These percentages per kilometer can be used in specifying the profiles of $LNO_x$ emissions in global models. In both regimes on average, only a small percentage of $LNO_x$ resides in the boundary layer following the convective event. A greater percentage of $LNO_x$ remains in the middle and upper troposphere where the $LNO_x$ was originally produced. These "backward C-shaped" average vertical distributions are in marked contrast to the C-shaped profiles calculated by *Pickering et al.* [1998] using 2-D cloud-resolving model simulations where a significant percentage of $LNO_x$ mass was transported to the boundary layer and relatively little $LNO_x$ mass was found between 1.5 and 6.5 km after convection concluded. Our results are similar to those from recent 3-D cloud models with explicit electrophysics. For example, *X. Zhang et al.* [2003a] found a maximum in $NO_x$ at mid-levels along with a secondary maximum at anvil levels indicating that a large portion of the $LNO_x$ remains within the cloud near the levels of its production.

[35] There are several reasons for the differences between the profiles calculated in this study and those presented by *Pickering et al.* [1998] which resulted in a C-shaped profile with peaks near the surface and in the upper troposphere. The profiles given by *Pickering et al.* [1998] were calculated using a 2-D cloud model with a much simpler treatment of $LNO_x$. In that model, $NO_x$ produced by CG flashes was distributed uniformly within the 20 dBz contour from the surface to −15°C while $NO_x$ produced by IC flashes was distributed uniformly from the −15°C isotherm to the cloud top. The 3-D CSCTM distributes $NO_x$ according to vertical distributions derived from observations of VHF sources associated with IC and CG flashes which are likely to be more realistic. *Pickering et al.* [1998] assumed the production scheme of *Price et al.* [1997] in which CG flashes produce 1100 moles NO per flash and IC flashes produce 110 moles NO per flash. A number of studies have contradicted this production scenario. Other explanations for the differences between the profiles presented here and those from *Pickering et al.* [1998] include the difficulty of realistically representing the complex wind structure of a thunderstorm in a 2-D model and the stronger reliance of the results of *Pickering et al.* [1998] on squall line simulations which may contain stronger vertical motions than other types of thunderstorms and thus be less representative.

[36] It should also be noted that our simulations indicate a small percentage of mass (∼1%) remains above the tropopause following convection, which results from overshooting transport of $LNO_x$ produced at lower altitudes. Individual modeling groups who implement these profiles may want to consider scaling these profiles so that mass is not directly injected into the stratosphere because most convective parameterizations used in larger-scale models do not produce overshooting cloud tops. Implementation of the profiles should involve scaling them to calculated cloud top height on an individual grid cell basis. Modeling groups may also want to consider where the profiles should be applied based on the cases included in this analysis. Of the midlatitude simulations, only the PRESTORM case was located south of 40°N. Those who apply these profiles in their own models may wish to consider applying the

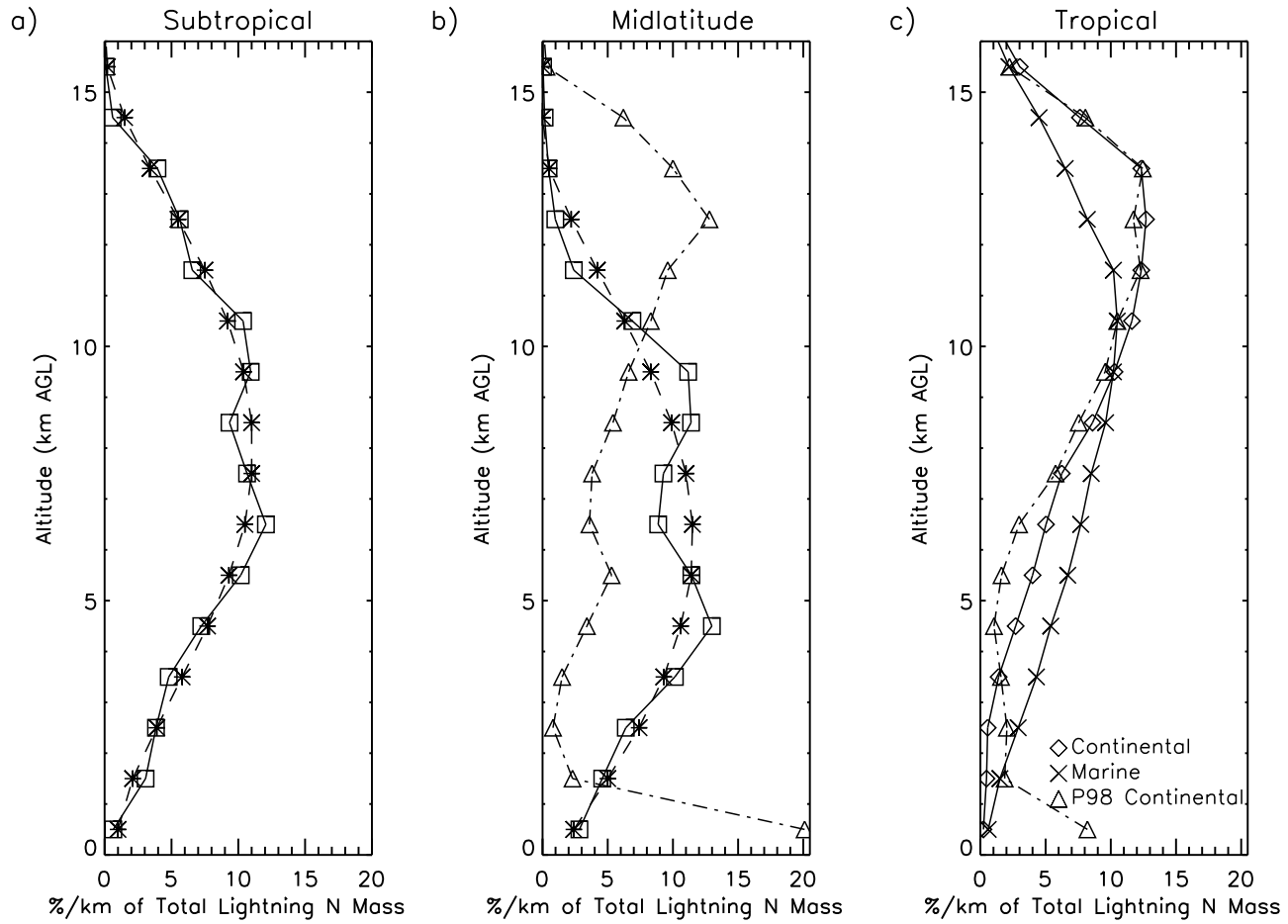


**Figure 12.** Average vertical distribution of percentage of $LNO_x$ mass per kilometer following convection (solid) for the (a) subtropical and (b) midlatitude continental regimes. Dashed line shows polynomial fit. Midlatitude continental profile from *Pickering et al.* [1998] (dash-dot) is also shown in Figure 12b. The hypothetical tropical marine profile (c) was created by extrapolating the subtropical average profile to a higher tropopause regime while the tropical continental profile was constructed using the *Pickering et al.* [1998] profile with the boundary layer maximum removed and that mass redistributed into layers from 4 to 11 km.

subtropical profile for grid cells as far north as 40°N in the Northern Hemisphere warm season (May through September) and as far south as 40°S in the Southern Hemisphere warm season (November through March). Additionally, the 10 and 12 July STERAO storms occurred at elevations of 1.6 km MSL while the PRESTORM and EULINOX storms were ~0.5 km MSL. We present profiles in Table 2 and Figure 12 for the percentage of $LNO_x$ mass per kilometer above ground level for consistency. Because of the elevation of the midlatitude cases, we urge modeling groups who implement these profiles to consider shifting the peak in the midlatitude profile higher by ~1 km.

[37] Assuming the density profile of the standard atmosphere, the total mass of $LNO_x$ was averaged over the EULINOX and STERAO storms. That amount of $NO_x$ distributed uniformly over a 200 km by 200 km region (typical of a global model grid cell) using the average midlatitude profile shown in Table 2 corresponds to a maximum increase in $NO_x$ mixing ratios of ~145 pptv between 7 and 9 km immediately following convection (~2 km higher than the maximum of the $LNO_x$ mass

**Table 2.** Average Profiles of $LNO_x$ Mass in Percent

| Altitude Range, km AGL | Subtropical | Midlatitude | Tropical | |
|---|---|---|---|---|
| | | | Continental | Marine |
| 0–1 | 1.0 | 2.4 | 0.2 | 0.6 |
| 1–2 | 2.1 | 5.0 | 0.5 | 1.5 |
| 2–3 | 3.9 | 7.4 | 0.6 | 2.9 |
| 3–4 | 5.8 | 9.3 | 1.4 | 4.3 |
| 4–5 | 7.7 | 10.6 | 2.7 | 5.4 |
| 5–6 | 9.3 | 11.4 | 4.0 | 6.7 |
| 6–7 | 10.5 | 11.5 | 5.0 | 7.7 |
| 7–8 | 11.0 | 11.0 | 6.2 | 8.5 |
| 8–9 | 11.0 | 9.9 | 8.6 | 9.6 |
| 9–10 | 10.4 | 8.3 | 10.3 | 10.2 |
| 10–11 | 9.2 | 6.3 | 11.6 | 10.5 |
| 11–12 | 7.5 | 4.2 | 12.4 | 10.2 |
| 12–13 | 5.5 | 2.2 | 12.7 | 8.2 |
| 13–14 | 3.4 | 0.5 | 12.4 | 6.5 |
| 14–15 | 1.5 | 0.0 | 7.6 | 4.5 |
| 15–16 | 0.2 | 0.0 | 3.0 | 2.2 |
| 16–17 | 0.0 | 0.0 | 0.8 | 0.5 |

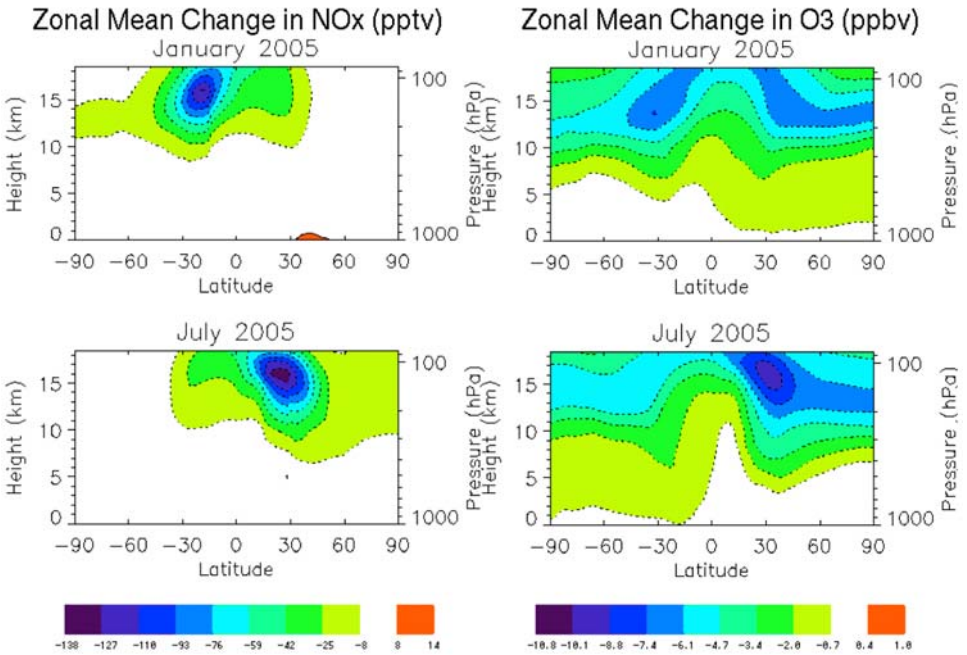


**Figure 13.** Zonal mean change in $NO_x$ (pptv) and $O_3$ (ppbv) in January and July resulting from using the lightning $NO_x$ profiles in Figure 11 instead of the profiles from *Pickering et al.* [1998].

distribution). Because the lifetime of $NO_x$ increases with altitude, $LNO_x$ will be converted to reservoir species such as PAN and $HNO_3$ more rapidly in the 7–9 km layer than at higher altitudes. As the time after convection increases, the maximum increase in $NO_x$ mixing ratios because of lightning would be seen at higher altitudes, which is consistent with the C-shaped profile of $NO_x$ typically observed in the troposphere. Downward transport from the stratosphere and aircraft emissions also contribute to the upper tropospheric maximum in observed $NO_x$ mixing ratios, while the maximum near the surface results from emissions from surface sources such as fossil fuel combustion and soil.

[38] The impact of assuming the vertical distributions of $LNO_x$ mass presented here has been calculated using NASA's Global Modeling Initiative (GMI) combined stratosphere-troposphere (Combo) CTM. The Combo CTM is detailed by *Ziemke et al.* [2006] and *Duncan et al.* [2007]. The tropospheric chemical mechanism includes 80 species and 300 reactions to simulate $O_3$-$NO_x$-hydrocarbon chemistry [*Bey et al.*, 2001]. Lightning is assumed to produce 5 Tg N $yr^{-1}$. Horizontal distribution of $LNO_x$ is determined by the locations of parameterized deep convection (as indicated by the upper tropospheric values of cloud mass flux) in the meteorological fields from the Global Modeling and Assimilation Office's GEOS-4 Data Assimilation System that are used to drive the Combo CTM. Flash rates are scaled such that on a regional and monthly basis they match those from the OTD/LIS climatology (D. J. Allen et al., Impact of lightning-NO emissions on North American photochemistry as determined using the GMI model, manuscript in preparation, 2009).

[39] Two one-year simulations were produced by the Combo CTM. The first used the vertical profiles of $LNO_x$ from *Pickering et al.* [1998] while the second simulation used the vertical profiles of $LNO_x$ shown in Figure 12a and b for the midlatitude and subtropical regimes. Because no tropical thunderstorms were simulated with the cloud and chemistry models, a hypothetical tropical distribution (Figure 12c) was constructed by extrapolating the subtropical profile to a higher tropopause regime. Test runs of the GMI Combo CTM revealed that this profile performed well in regions dominated by marine convection, but in tropical continental areas the *Pickering et al.* [1998] profile yielded better results for upper tropospheric ozone compared with ozonesonde data. Therefore, in tropical continental regions the *Pickering et al.* [1998] profile, modified by removing the boundary layer maximum and redistributing this mass between 4 and 11 km, was used. The tropical profiles are also provided in Table 2.

[40] Figure 13 shows the zonal mean change in $NO_x$ and $O_3$ in January and July when the profiles shown in Figure 12 are used instead of the *Pickering et al.* [1998] profiles. Because these profiles place less NO in the upper troposphere, $NO_x$ decreases above 10 km with decreases of over 100 pptv found over the Southern Hemisphere in January and over the Northern Hemisphere in July. The decreases in $NO_x$ in the upper troposphere, which results from using the modified vertical profiles of $LNO_x$ mass, also cause a small decrease in ozone throughout much of the troposphere. The largest decrease in ozone is ~10 ppbv in July at 15 km and 30°N. The changes resulting from the use of different vertical distributions of $LNO_x$ are typical of other seasons not shown. In October, the pattern of $NO_x$ and ozone decrease is similar to that of July, though the ozone decrease in the Northern Hemisphere is greater in October. In April, $NO_x$ decreases are smaller than in other months (<60 pptv) and the peak ozone decreases (~7 ppbv) focused in the Southern Hemisphere.

[41] It should be noted that a number of studies have assumed vertical distributions of lightning NO that are different from those presented here and have found reasonable comparison with available observations. For example,

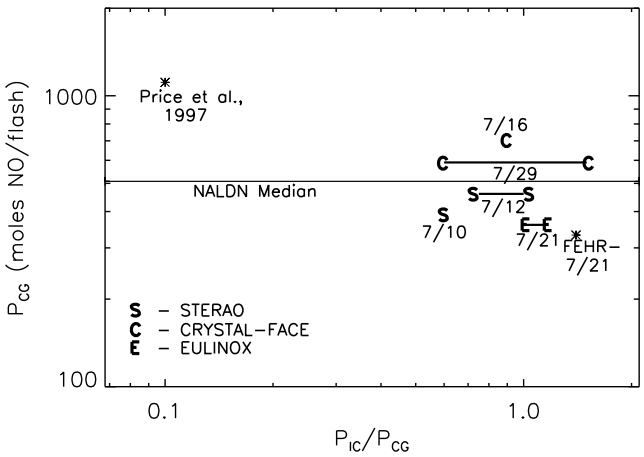


**Figure 14.** Estimated $LNO_x$ production scenarios for the 16 July CRYSTAL-FACE (C, 7/16), 29 July CRYSTAL-FACE (C, 7/29), 10 July STERAO (S, 7/10), 12 July STERAO (S, 7/12), and 21 July EULINOX (E, 7/21) storms. The bars in the 7/29 CRYSTAL-FACE, 7/12 STERAO, and 7/21 EULINOX storms indicate the estimate uncertainty. The *Price et al.* [1997] and *Fehr et al.* [2004] production scenarios are indicated by asterisks, while the estimated value of $P_{CG}$ calculated assuming the NALDN median peak current from *Orville et al.* [2002] is indicated by the horizontal line.

both *Tie et al.* [2001] and *R. Zhang et al.* [2003] assumed that $LNO_x$ was distributed uniformly below the convective cloud top height and found reasonable agreement with observations obtained during several field projects. *Hudman et al.* [2007] assumed the *Pickering et al.* [1998] vertical distributions and were able to reproduce aircraft observations obtained over North America during the International Consortium on Atmospheric Transport and Transformation (ICARTT) campaign after adjusting the amount of NO produced per flash. *Labrador et al.* [2005] evaluated several different vertical distributions of lightning NO including uniform mixing ratio increases (as assumed by *Tie et al.* [2001] and *R. Zhang et al.* [2003]), the *Pickering et al.* [1998] profiles, and distributing all $LNO_x$ into the five uppermost layers of cloud. They were unable to identify a single best vertical distribution scheme because of the large amount of scatter in the observational data sets obtained during different field projects.

### 4.2. NO Production

[42] A best fit production scenario of $P_{IC}$ and $P_{CG}$ has been estimated by comparing in-cloud aircraft observations with model output for the five storms where in-cloud aircraft observations were available. Figure 14 shows the production scenarios estimated for these five storms as well as the production scenario from *Price et al.* [1997], which was used in calculating the vertical profiles of $LNO_x$ mass presented by *Pickering et al.* [1998] and has been used in many global CTMs. In all cases, $P_{CG}$ was estimated to be less than the 1100 moles per CG flash given by *Price et al.* [1997]. In addition, in all cases the ratio of $P_{IC}$ to $P_{CG}$ was greater than the commonly assumed value of 0.1 presented by *Price et al.* [1997]. Over the five storms simulated, the average estimated $P_{CG}$ was 500 moles NO per flash or 7 kg N per flash (range of 360–700 moles per flash or ~5–9.8 kg N per flash). Assuming $P_{IC}/P_{CG}$ ratios in the middle of the estimated uncertainty ranges for the 29 July CRYSTAL-FACE, 12 July STERAO, and 21 July EULINOX storms yields an average $P_{IC}/P_{CG}$ ratio of 0.93, corresponding to 465 moles NO. The median peak current (16.5 kA for negative flashes and 19.8 kA for positive flashes, which account for 10.9% of the total) of the North American Lightning Detection Network (NALDN) presented by *Orville et al.* [2002] corresponds to a $P_{CG}$ value of 508 moles NO when using the *DeCaria et al.* [2000] relationship between peak current and energy dissipated, which agrees well with our estimate of 500 moles NO per CG flash. Therefore, the cases we have simulated appear to be representative of midlatitude and subtropical lightning. Assuming the average production scenario over the five storms presented, an average global IC-to-CG ratio of three (the same as estimated for the continental United States by *Boccippio et al.* [2001]), and a global flash rate of 44 flashes $s^{-1}$ [*Christian et al.*, 2003] yields a global lightning NO source of 8.6 Tg N $yr^{-1}$.

[43] Estimates of the global lightning NO source have ranged from 2 to 20 Tg N $yr^{-1}$ [*IPCC*, 2001]. This range has been narrowed in recent years. *IPCC* [2007] recommends a 1.1–6.4 Tg N $yr^{-1}$ range, though a more comprehensive review has specified the range to be 2–8 Tg N $yr^{-1}$ [*Schumann and Huntrieser*, 2007]. This review considered all of the methods of estimating $LNO_x$ production: global model estimates constrained by various observations, cloud-resolved modeling studies, aircraft measurements, laboratory experiments, and theoretical estimates. Our estimate of 8.6 Tg N $yr^{-1}$ lies near the upper end of the recently established range of global estimates. It is unlikely that our estimate is larger than values in this range due to the global extrapolation. Because of satellite observations of total lightning activity from instruments such as the Optical Transient Detector (OTD; see *Christian et al.* [2003]), uncertainty in the global flashrate has been greatly reduced. Perhaps more likely it is because of the fact that our average production scenario was calculated using data from only midlatitude continental and subtropical storms. No tropical thunderstorms were simulated in this analysis. Because 78% of lightning flashes occur between 30°S and 30°N [*Christian et al.*, 2003], further investigation of the properties of tropical lightning flashes and their production of NO is needed. On the basis of analysis of data from the TROCCINOX experiment in Brazil, *Huntrieser et al.* [2008] suggest that tropical flashes (shorter, possibly due to low vertical wind shear) produce less $LNO_x$ than subtropical or midlatitude flashes (longer, possibly due to greater wind shear). If this hypothesis holds true throughout the tropics, inclusion of tropical events into our average production scenario will decrease this average value. Tropical event simulations are currently underway. We urge modeling groups who wish to adapt our production per flash estimates to global models to use caution when applying these estimates to the tropics. In this region, the results should be thoroughly validated against available $NO_x$ and ozone observations and the production per flash reduced, if necessary, to reproduce observed trace gas distributions.

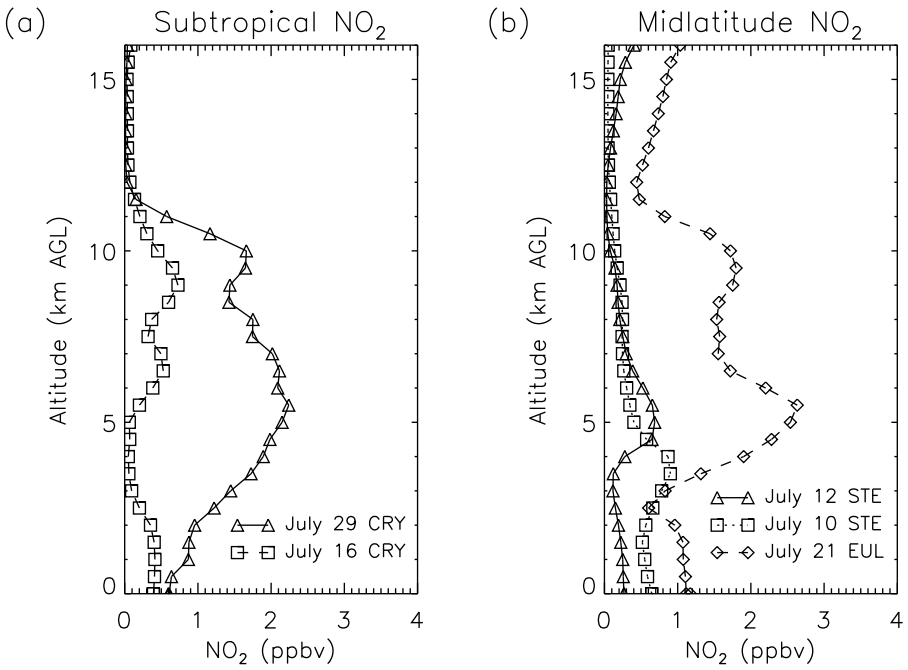


**Figure 15.** Average vertical profiles of $NO_2$ mixing ratio in the convective core region following (a) simulated subtropical storms and (b) midlatitude storms.

[44] In part on the basis of the work presented here, several modeling studies have assumed a production scenario similar to the mean scenario presented here where both IC and CG flashes produce on average approximately 500 moles NO per flash. These works provide important information on the application of results presented here and comparisons with data sets not included in this study. *Hudman et al.* [2007] simulated $NO_x$ over the United States during the ICARTT campaign using the GEOS-Chem CTM and found that assuming a production per flash of 500 moles NO instead of the default GEOS-Chem value of 125 moles NO improved the comparison with upper tropospheric aircraft observations. *Cooper et al.* [2006] simulated $LNO_x$ production and transport over North America during the same period using the FLEXPART model and assumed IC and CG flashes produce 460 moles NO (on the basis of the *DeCaria et al.* [2005] results for the 12 July STERAO storm) and a 2-day lifetime for upper tropospheric $NO_x$. Resulting ozone enhancements were estimated with a box model. The results showed a good agreement between simulated $NO_x$ and DC-8 aircraft observations and between simulated ozone enhancements and observations from commercial aircraft and ozonesondes. *Jourdain et al.* [2009] found that assuming a production per flash of 520 moles NO (rather than 260 moles NO) in GEOS-Chem simulations of ozone over the United States substantially reduced the model's bias relative to TES observations.

### 4.3. $NO_2$ in the Vicinity of Electrified Storms

[45] A number of recent studies have attempted to constrain the magnitude of the global $LNO_x$ source using satellite observations. *Beirle et al.* [2004] used correlations between GOME $NO_2$ column densities and data from the Lightning Imaging Sensor (LIS) to estimate that lightning produces 2.8 Tg N $yr^{-1}$ though the range of uncertainty was large (0.8–14 Tg N $yr^{-1}$). *Beirle et al.* [2006] also studied $LNO_x$ production in the Gulf of Mexico using GOME data and NLDN observations and found that lightning produced 90 moles NO per flash in this region. If extrapolated to the global scale, this value corresponds to a $LNO_x$ source of 1.7 Tg N $yr^{-1}$ with a range of uncertainty from 0.6 to 4.7 Tg N $yr^{-1}$. *Boersma et al.* [2005] used GOME $NO_2$ observations and a global CTM with two different $LNO_x$ paramaterizations and concluded that $LNO_x$ production was between 1.1 and 6.4 Tg N $yr^{-1}$. *Martin et al.* [2007] used GEOS-Chem simulations in conjunction with space-based observations of $NO_x$, ozone, and nitric acid to estimate $LNO_x$ production of 6 ± 2 Tg N $yr^{-1}$. *Beirle et al.* [2009] have demonstrated through use of cloud/chemistry model output and radiative transfer modeling for a typical marine convective system that nadir-viewing satellites likely have a sensitivity of slightly under 50% for $LNO_x$. Therefore, estimates of $LNO_x$ from satellites need to take this sensitivity factor into consideration.

[46] $NO_2$ profiles appropriate for regions dominated by $NO_x$ from lightning are useful for improving satellite retrievals of $NO_2$ column amounts in such environments. The air mass factor used in converting satellite-measured slant columns to vertical columns of $NO_2$ is highly dependent on the $NO_2$ profile shape. $NO_2$ profiles from the version of the CSCTM that includes chemical production and loss have been used to examine the structure of this species in the CRYSTAL-FACE, STERAO, and EULINOX storms.

[47] Mean vertical profiles of $NO_2$ after convection are shown in Figure 15. The profiles were calculated over a 40 × 40 $km^2$ area positioned in the convective core region of the model domain. The 29 July profile shows extremely

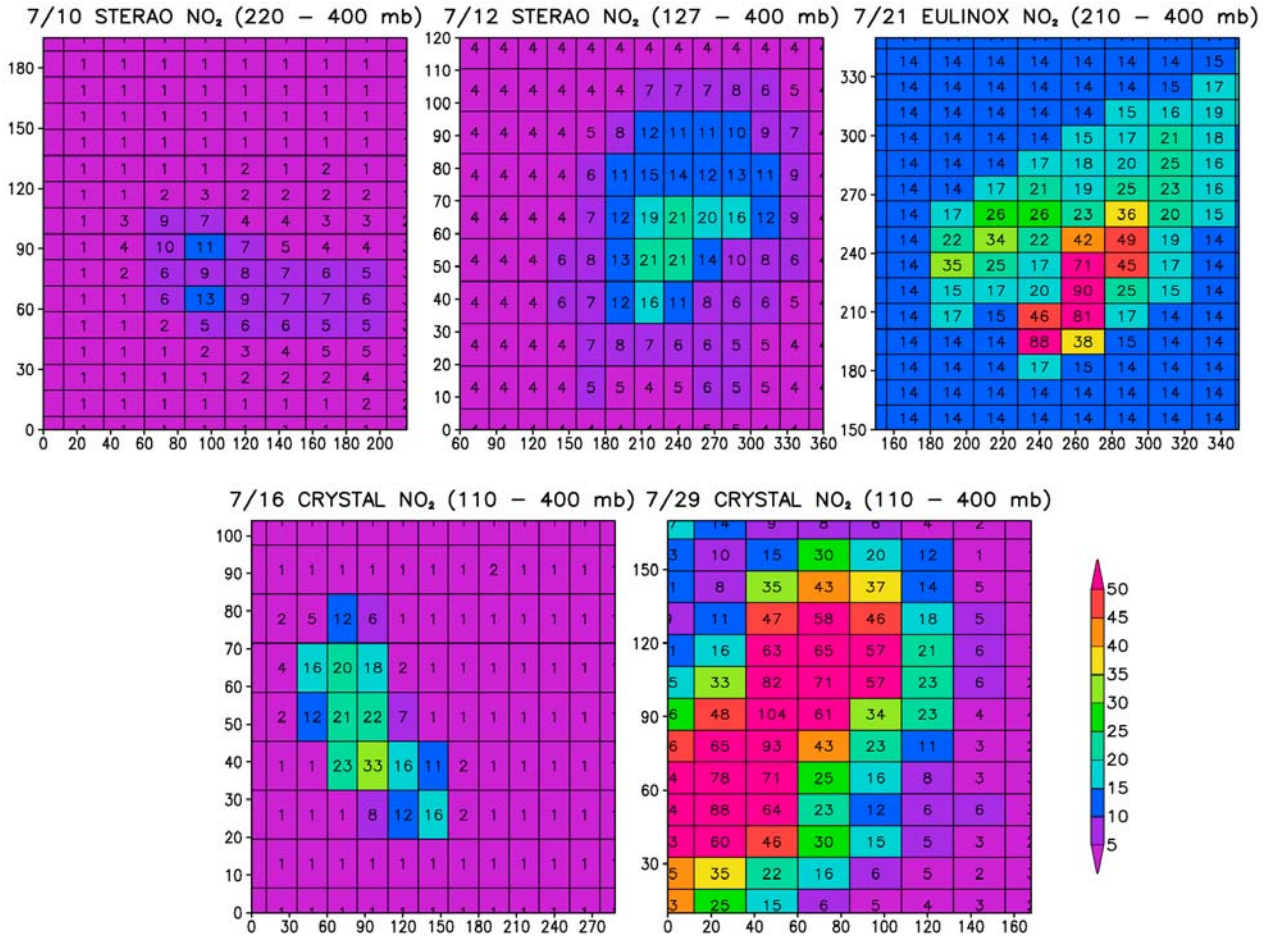


**Figure 16.** Partial $NO_2$ columns ($10^{14}$ molecules $cm^{-2}$) from the tropopause to 400 hPa for CRYSTAL-FACE, STERAO, and EULINOX simulated thunderstorms.

elevated $NO_2$ mixing ratios exceeding 2 ppbv from 5 to 7.5 km, while the 16 July profile maximizes at only 0.7 ppbv at 9.5 km. The disparity in profiles is because of the large difference in flash rates in the two storms with over 4000 CG flashes recorded by the NLDN in the 29 July storm, and only 301 CG flashes recorded in the 16 July storm. Of the midlatitude storms, the vertical profile of $NO_2$ from the EULINOX storm (with both high flash rate and pollution inflow) is much larger than in either of the STERAO storms with a maximum of nearly 3 ppbv at 5.5 km.

[48] In addition to $NO_2$ profiles, we have also used these simulations to estimate partial columns of $NO_2$ that a satellite may be able to observe in the upper portion of a convective cloud. *Vasilkov et al.* [2008] compared cloud top pressures retrieved in the UV wavelengths by the Ozone Monitoring Instrument (OMI) aboard the Aura satellite with those retrieved by IR measurements from MODIS aboard Aqua. A comparison of both cloud top pressure products with CloudSat radar observations indicate that OMI may be able to measure $NO_2$ as far down as 400–600 mbar in the presence of deep convective clouds. Partial $NO_2$ columns were calculated for our storms of interest by averaging 2 km model output over 13 × 24 $km^2$ areas equivalent to OMI's nadir footprint and integrating the column from 400 mbar to the tropopause. The results are shown in Figure 16. The 29 July CRYSTAL-FACE and 21 July EULINOX storms show the greatest degree of enhancement, which is consistent with the $NO_2$ profiles shown in Figure 15. In the 29 July CRYSTAL-FACE storm, the region of highly elevated $NO_2$ columns extends over 100 km. Table 3 shows the sensitivity of the peak and background $NO_2$ columns to the choice of column depth. The peak values indicate the maximum partial $NO_2$ column amounts over an OMI grid box area (13 × 24 $km^2$) in the storm anvil or core regions, while the background values indicate the mean partial $NO_2$ column amounts outside of the storm region. These data should be useful in providing a range of values of tropo-

**Table 3.** Partial $NO_2$ Columns From the Tropopause to 400, 500, and 600 mbar[a]

| | Tropopause to 400 mbar | | Tropopause to 500 mbar | | Tropopause to 600 mbar | |
|---|---|---|---|---|---|---|
| Storm | Peak | Background | Peak | Background | Peak | Background |
| July 16 CRY | 33 | 1 | 48 | 1 | 54 | 2 |
| July 29 CRY | 104 | 3 | 159 | 3 | 223 | 4 |
| July 10 STE | 13 | 1 | 21 | 1 | 40 | 1 |
| July 12 STE | 21 | 4 | 24 | 5 | 24 | 5 |
| July 21 EUL | 90 | 14 | 140 | 16 | 192 | 17 |

[a]Values are given in $10^{14}$ molecules $cm^{-2}$.

spheric column $NO_2$ that may be compared to retrievals over convective clouds from such instruments as OMI.

## 5. Conclusions

[49] Simulations of six midlatitude and subtropical thunderstorms monitored during four field projects have been conducted using the CSCTM, which includes a parameterized source of $LNO_x$. To estimate $LNO_x$ production per flash in each storm, different scenarios of $P_{IC}$ and $P_{CG}$ were specified in the model, and the results compared with in-cloud aircraft observations of $NO_x$. The results suggest that $P_{IC}$ may be nearly the same as $P_{CG}$. A frequent assumption that $P_{IC}$ is equal to one tenth $P_{CG}$ resulted in a significant underestimation of $LNO_x$ in the five simulations where anvil observations were available. We echo the recommendation of *Ridley et al.* [2005] for use of comparable values of $P_{CG}$ and $P_{IC}$. The *Ridley et al.* [2005] recommendation was partly on the basis of one of the cases presented here. Our similar results for four additional cases strengthen this recommendation. The mean $P_{CG}$ obtained from the five case simulations is 500 moles NO per flash (range 360–700) with a mean $P_{IC}/P_{CG}$ ratio of 0.93, which, when extrapolated globally, yields an estimate at the high end of the currently accepted range. This may result from the absence of tropical flashes in this analysis.

[50] Vertical profiles of the percentage of $LNO_x$ mass in each 1-km layer after the convection show very little $LNO_x$ mass near the surface with the majority of $LNO_x$ remaining in the middle and upper troposphere in a "backward C-shaped" profile. Global and regional CTMs that have adopted C-shaped vertical profiles of $LNO_x$ mass may be underestimating the amount of $LNO_x$ in the mid- troposphere and overestimating the amount near the surface. Global models which are changed to represent equivalent per flash production by IC and CG lightning may require a change of the global $LNO_x$ source strength to reasonably reproduce $NO_x$ observations in the middle and upper troposphere. Changes in the vertical placement of $LNO_x$ in CTMs may significantly alter distributions of species such as $O_3$ and OH.

[51] It should be noted that this study is based on simulations of six midlatitude and subtropical thunderstorms. The mean peak current of CG flashes in these cases was approximately equal to the North American median value which suggests that the cases we have simulated are representative of lightning in this region. Because such observations are not available globally and the energy dissipated by IC flashes remains highly uncertain, we cannot conclude with certainty that the results are representative of lightning in all regions. This analysis did not include any tropical thunderstorms though simulations of tropical cases are currently in progress. For these reasons, we urge modeling groups to use caution when extrapolating these results to the global scale. Application of both the mean production per flash and the vertical distributions of $LNO_x$ must be carefully evaluated in different regions through comparison with available satellite, ground- and aircraft-based data.

[52] **Acknowledgments.** The authors would like to acknowledge the contribution of the following individuals who provided observational data: Jimena Lopez and Max Loewenstein from NASA Ames Research Center; Eric Richard from NOAA Earth System Research Laboratory; Jim Dye and Mary Barth from NCAR; Heidi Huntrieser and Hartmut Höller from Deutsches Zentrum für Luft- und Raumfahrt. The authors also wish to thank Donghai Wang, formerly of NASA Langley Research Center, for providing the ARPS simulation of the 16 July CRYSTAL-FACE storm.

## References

Allen, D. J., and K. E. Pickering (2002), Evaluation of lightning flash rate parameterizations for use in a global chemical-transport model, *J. Geophys. Res.*, *107*(D23), 4711, doi:10.1029/2002JD002066.

Barth, M. C., et al. (2007), Cloud-scale model intercomparison of chemical constituent transport in deep convection, *Atmos. Chem. Phys.*, *7*, 4709–4731.

Barthe, C., and M. C. Barth (2008), Evaluation of a new lightning-produced $NO_x$ parameterization for cloud resolving models and its associated uncertainties, *Atmos. Chem. Phys.*, *8*, 4691–4710.

Beirle, S., U. Platt, M. Wenig, and T. Wagner (2004), $NO_x$ production by lightning estimated with GOME, *Adv. Space Res.*, *34*(4), 793–797, doi:10.1016/j.asr.2003.07.069.

Beirle, S., et al. (2006), Estimating the $NO_x$ produced by lightning from GOME and NLDN data: A case study in the Gulf of Mexico, *Atmos. Chem. Phys.*, *6*, 1075–1089.

Beirle, S., M. Salzmann, M. G. Lawrence, and T. Wagner (2009), Sensitivity of satellite observations for freshly produced lightning $NO_x$, *Atmos. Chem. Phys.*, *9*, 1077–1094.

Bey, I., D. J. Jacob, R. M. Yantosca, J. A. Logan, B. D. Field, A. M. Fiore, Q. Li, H. Y. Liu, L. J. Mickley, and M. G. Schultz (2001), Global modeling of tropospheric chemistry with assimilated meteorology: Model description and evaluation, *J. Geophys. Res.*, *106*(D19), 23,073–23,095, doi:10.1029/2001JD000807.

Boccippio, D. J., K. L. Cummins, H. J. Christian, and S. J. Goodman (2001), Combined satellite- and surface-based estimation of the intracloud-cloud-to-ground lightning ratio over the continental United States, *Mon. Weather Rev.*, *129*, 108–122, doi:10.1175/1520-0493(2001)129<0108:CSASBE>2.0.CO;2.

Boersma, K. F., H. J. Eskes, E. W. Meijer, and H. M. Kelder (2005), Estimates of lightning $NO_x$ production from GOME satellite observations, *Atmos. Chem. Phys.*, *5*, 2311–2331.

Chameides, W. L. (1986), The role of lightning in the chemistry of the atmosphere, in *The Earth's Electrical Environment, Studies in Geophysics*, pp. 70–77, Natl. Acad. Press, Washington, D. C.

Christian, H. J., et al. (2003), Global frequency and distribution of lightning as observed from space by the Optical Transient Detector, *J. Geophys. Res.*, *108*(D1), 4005, doi:10.1029/2002JD002347.

Cooper, O. R., et al. (2006), Large upper tropospheric ozone enhancements above midlatitude North America during summer: In situ evidence from the IONS and MOZAIC ozone measurement network, *J. Geophys. Res.*, *111*, D24S05, doi:10.1029/2006JD007306.

Cooray, G. V. (1997), Energy dissipation in lightning flashes, *J. Geophys. Res.*, *102*, 21,401–21,410, doi:10.1029/96JD01917.

Cummins, K. L., M. J. Murphy, E. A. Bardo, W. L. Hiscox, R. B. Pyle, and A. E. Pifer (1998), A combined TOA/MDF technology upgrade of the U.S. National Lightning Detection Network, *J. Geophys. Res.*, *103*, 9035–9044, doi:10.1029/98JD00153.

DeCaria, A. J., K. E. Pickering, G. L. Stenchikov, J. R. Scala, J. L. Stith, J. E. Dye, B. A. Ridley, and P. Laroche (2000), A cloud-scale model study of lightning-generated $NO_X$ in an individual thunderstorm during STERAO-A, *J. Geophys. Res.*, *105*, 11,601–11,616, doi:10.1029/2000JD900033.

DeCaria, A. J., K. E. Pickering, G. L. Stenchikov, and L. E. Ott (2005), Lightning-generated $NO_x$ and its impact on tropospheric ozone production: A three-dimensional modeling study of a stratosphere-troposphere experiment: Radiation, aerosols, and ozone (STERAO-A) thunderstorm, *J. Geophys. Res.*, *110*, D14303, doi:10.1029/2004JD005556.

Duncan, B. N., S. E. Strahan, Y. Yoshida, S. D. Steenrod, and N. Livesey (2007), Model study of the cross-tropopause transport of biomass burning pollution, *Atmos. Chem. Phys.*, *7*, 3713–3736.

Dye, J. E., et al. (2000), An overview of the STERAO-Deep convection experiment with results for the 10 July Storm, *J. Geophys. Res.*, *105*, 10,023–10,045, doi:10.1029/1999JD901116.

Fehr, T., H. Höller, and H. Huntrieser (2004), Model study on production and transport of lightning-produced $NO_x$ in a EULINOX supercell storm, *J. Geophys. Res.*, *109*, D09102, doi:10.1029/2003JD003935.

Gallardo, L., and V. Cooray (1996), Could cloud-to-cloud discharges be as effective as cloud-to-ground discharges in producing $NO_x$?, *Tellus*, *48B*, 641–651.

Höller, H., H. Huntrieser, C. Feigl, C. Théry, P. Laroche, U. Finke, and J. Seltmann (2000), The severe storms of 21 July 1998—Evolution and Implications for $NO_x$-production, in *EULINOX—The European Lightning*

*Nitrogen Oxides Experiment*, edited by H. Höller and U. Schumann, *Rep. DLR-FB 2000–28*, pp. 109–128, Deutches Zentrum für Luft- und Raumfahrt, Köln.

Holmes, C., M. Brook, P. Krehbiel, and R. McRory (1971), On the power spectrum and mechanism of thunder, *J. Geophys. Res.*, *76*, 2106–2115, doi:10.1029/JC076i009p02106.

Hudman, R. C., et al. (2007), Surface and lightning sources of nitrogen oxides over the United States: Magnitudes, chemical evolution, and outflow, *J. Geophys. Res.*, *112*, D12S05, doi:10.1029/2006JD007912.

Huntrieser, H., et al. (2002), Airborne measurements of $NO_x$, tracer species, and small particles during the European Lightning Nitrogen Oxides Experiment, *J. Geophys. Res.*, *107*(D11), 4113, doi:10.1029/2000JD000209.

Huntrieser, H., U. Schumann, H. Schlager, H. Höller, A. Giez, H.-D. Betz, D. Brunner, C. Forster, O. Pinto Jr., and R. Calheiros (2008), Lightning activity in Brazilian thunderstorms during TROCCINOX: Implications for $NO_x$ production, *Atmos. Chem. Phys.*, *8*, 921–953.

Intergovernmental Panel on Climate Change (IPCC) (2001), Climate Change 2001: The Scientific Basis, in *Contribution of Working Group I to the Third Assessment Report of the Intergovernmental Panel on Climate Change*, edited by J. T. Houghton et al., Cambridge Univ. Press, Cambridge, U. K.

Intergovernmental Panel on Climate Change (IPCC) (2007), Climate Change 2007: Synthesis Report, in *Contribution of Working Group I to the Fourth Assessment Report of the Intergovernmental Panel on Climate Change*, edited by S. Solomon et al., Cambridge Univ. Press, Cambridge, U. K.

Johnson, R. H., and P. J. Hamilton (1988), The relationship of surface pressure features to the precipitation and airflow structure of an intense midlatitude squall line, *Mon. Weather Rev.*, *116*, 1444–1472, doi:10.1175/1520-0493(1988)116<1444:TROSPF>2.0.CO;2.

Jourdain, L., S. S. Kulawik, H. M. Worden, K. E. Pickering, J. Worden, and A. M. Thompson (2009), Lightning $NO_x$ emissions over the USA investigated using TES, NLDN, LRLDN, IONS data and the GEOS-Chem model, *Atmos. Chem. Phys. Discuss.*, *9*, 1123–1155.

Labrador, L. J., R. von Kuhlmann, and M. G. Lawrence (2004), Strong sensitivity of the global mean OH concentration and the tropospheric oxidizing efficiency to the source of $NO_x$ from lightning, *Geophys. Res. Lett.*, *31*(6), L06102, doi:10.1029/2003GL019229.

Labrador, L. J., R. von Kuhlmann, and M. G. Lawrence (2005), The effects of lightning-produced $NO_x$ and its vertical distribution on atmospheric chemistry: Sensitivity simulations with MATCH-MPIC, *Atmos. Chem. Phys.*, *5*, 1815–1834.

Lopez, J. P., et al. (2006), CO signatures in subtropical convective clouds and anvils during CRYSTAL-FACE: An analysis of convective transport and entrainment using observations and a cloud-resolving model, *J. Geophys. Res.*, *111*, D09305, doi:10.1029/2005JD006104.

MacGorman, D. R., and W. D. Rust (1998), *The Electrical Nature of Storms*, 422 pp., Oxford Univ. Press, Oxford.

Madronich, S. (1987), Photodissociation in the atmosphere 1. Actinic flux and the effects of ground reflections and clouds, *J. Geophys. Res.*, *92*(D8), 9740–9752, doi:10.1029/JD092iD08p09740.

Maggio, C. R., T. C. Marshall, and M. Stolzenburg (2009), Estimations of charge transferred and energy released by lightning flashes, *J. Geophys. Res.*, *114*, D14203, doi:10.1029/2008JD011506.

Martin, R. V., B. Sauvage, I. Folkins, C. E. Sioris, C. Boone, P. Bernath, and J. Ziemke (2007), Space-based constraints on the production of nitric oxide by lightning, *J. Geophys. Res.*, *112*, D09309, doi:10.1029/2006JD007831.

Nielsen, K. E., R. A. Maddox, and S. V. Vasiloff (1994), The evolution of cloud-to-ground lightning within a portion of the 10–11 June 1985 Squall Line, *Mon. Weather Rev.*, *122*, 1809–1817, doi:10.1175/1520-0493(1994)122<1809:TEOCTG>2.0.CO;2.

Orville, R. E., G. R. Huffines, W. R. Burrows, R. L. Holle, and K. L. Cummins (2002), The North American Lightning Detection Network (NALDN)—First Results: 1998–2000, *Mon. Weather Rev.*, *130*(8), 2098–2109, doi:10.1175/1520-0493(2002)130<2098:TNALDN>2.0.CO;2.

Ott, L. E., K. E. Pickering, G. L. Stenchikov, H. Huntrieser, and U. Schumann (2007), Effects of lightning $NO_x$ production during the 21 July European Lightning Nitrogen Oxides Project storm studied with a three-dimensional cloud-scale chemical transport model, *J. Geophys. Res.*, *112*, D05307, doi:10.1029/2006JD007365.

Pickering, K. E., Y. Wang, W.-K. Tao, C. Price, and J.-F. Müller (1998), Vertical distributions of lightning $NO_x$ for use in regional and global chemical transport models, *J. Geophys. Res.*, *103*, 31,203–31,216, doi:10.1029/98JD02651.

Price, C., J. Penner, and M. Prather (1997), $NO_x$ from lightning 1. Global distributions based on lightning physics, *J. Geophys. Res.*, *102*, 5929–5941, doi:10.1029/96JD03504.

Rahman, M., V. Cooray, V. A. Rakov, M. A. Uman, P. Liyanage, B. A. DeCarlo, J. Jerauld, and R. C. Olsen III (2007), Measurements of $NO_x$ produced by rocket-triggered lightning, *Geophys. Res. Lett.*, *34*, L03816, doi:10.1029/2006GL027956.

Ridley, B., et al. (2004), Florida thunderstorms: A faucet of reactive nitrogen to the upper troposphere, *J. Geophys. Res.*, *109*, D17305, doi:10.1029/2004JD004769.

Ridley, B., K. Pickering, and J. Dye (2005), Comments on the parameterization of lightning-produced NO in global chemistry-transport models, *Atmos. Environ.*, *39*, 6184–6187, doi:10.1016/j.atmosenv.2005.06.054.

Rutledge, S. A., and D. R. MacGorman (1988), Cloud-to-ground lightning activity in the 10–11 June 1985 mesoscale convective system observed during the Oklahoma-Kansas PRE-STORM project, *Mon. Weather Rev.*, *116*, 1393–1408, doi:10.1175/1520-0493(1988)116<1393:CTGLAI>2.0.CO;2.

Rutledge, S. A., R. A. Houze Jr., M. I. Biggerstaff, and T. Matejka (1988), The Oklahoma-Kansas mesoscale convective system of 10–11 June 1985: Precipitation structure and single-Doppler radar analysis, *Mon. Weather Rev.*, *116*, 1409–1430, doi:10.1175/1520-0493(1988)116<1409:TOMCSO>2.0.CO;2.

Schumann, U., and H. Huntrieser (2007), The global lightning-induced nitrogen oxides source, *Atmos. Chem. Phys.*, *7*, 3823–3907.

Skamarock, W. C., et al. (2000), Numerical simulations of the July 10 stratospheric-tropospheric experiment: Radiation, aerosols, and ozone/deep convection experiment convective system: Kinematics and transport, *J. Geophys. Res.*, *105*(D15), 19,973–19,990, doi:10.1029/2000JD900179.

Skamarock, W. C., J. E. Dye, E. Defer, M. C. Barth, J. L. Stith, B. A. Ridley, and K. Baumann (2003), Observational- and modeling-based budget of lightning-produced $NO_x$ in a continental thunderstorm, *J. Geophys. Res.*, *108*(D10), 4305, doi:10.1029/2002JD002163.

Stamnes, K., S.-C. Tsay, W. Wiscombe, and K. Jayaweera (1988), Numerically stable algorithm for discrete-ordinate method radiative transfer in multiple scattering and emitting layered media, *Appl. Opt.*, *27*, 2502–2509, doi:10.1364/AO.27.002502.

Stenchikov, G. L., K. Pickering, A. DeCaria, W.-K. Tao, J. Scala, L. Ott, D. Bartels, and T. Matejka (2005), Simulation of the fine structure of the 12 July 1996 stratosphere-troposphere experiment: Radiation, aerosols and ozone (STERAO-A) storm accounting for effects of terrain and interaction with mesoscale flow, *J. Geophys. Res.*, *110*, D14304, doi:10.1029/2004JD005582.

Stockwell, D. Z., C. Giannakopoulos, P.-H. Plantevin, G. D. Carver, M. P. Chipperfield, K. S. Law, J. A. Pyle, D. E. Shallcross, and K.-Y. Wang (1999), Modelling $NO_x$ from lightning and its impact on global chemical fields, *Atmos. Environ.*, *33*, 4477–4493, doi:10.1016/S1352-2310(99)00190-9.

Tao, W.-K., and J. Simpson (1993), Goddard cumulus ensemble model. Part I: Model description, *Terr., Atmos, Oceanic Sci.*, *4*, 35–72.

Tao, W.-K., et al. (2003a), Microphysics, radiation and surface processes in the goddard cumulus ensemble (GCE) model, *Meteorol. Atmos. Phys.*, *82*, 97–137, doi:10.1007/s00703-001-0594-7.

Tao, W.-K., et al. (2003b), Regional-scale modeling at NASA Goddard Space Flight Center, *Research Signpost Recent Res. Dev. Atmos. Sci.*, *2*, 1–52.

Tie, X., R. Zhang, G. Brasseur, L. Emmons, and W. Lei (2001), Effects of lightning on reactive nitrogen and nitrogen reservoir species in the troposphere, *J. Geophys. Res.*, *106*(D3), 3167–3178.

Vasilkov, A., J. Joiner, R. Spurr, P. K. Bhartia, P. Levelt, and G. Stephens (2008), Evaluation of the OMI cloud pressures derived from rotational Raman scattering by comparisons with other satellite data and radiative transfer simulations, *J. Geophys. Res.*, *113*, D15S19, doi:10.1029/2007JD008689.

Wang, Y., A. W. DeSilva, G. C. Goldenbaum, and R. R. Dickerson (1998), Nitric oxide production by simulated lightning: Dependence on current, energy, and pressure, *J. Geophys. Res.*, *103*(D15), 19,149–19,159, doi:10.1029/98JD01356.

Xue, M., K. K. Droegemeier, and V. Wong (2000), The Advanced Regional Prediction System (ARPS)—A multiscale non-hydrostatic atmospheric simulation and prediction tool. Part I: Model dynamics and verification, *Meteorol. Atmos. Phys.*, *75*, 161–193, doi:10.1007/s007030070003.

Xue, M., K. K. Droegemeier, V. Wong, A. Shapiro, K. Brewster, F. Carr, D. Weber, Y. Liu, and D.-H. Wong (2001), The Advanced Regional Prediction System (ARPS)—A multiscale non-hydrostatic atmospheric simulation and prediction tool. Part II: Model physics and applications, *Meteorol. Atmos. Phys.*, *76*, 134–165, doi:10.1007/s007030170027.

Zhang, R. Y., X. X. Tie, and D. W. Bond (2003), Impacts of anthropogenic and natural NOx sources over the U.S. on tropospheric chemistry, *Proc. Natl. Acad. Sci. U. S. A.*, *100*, 1505–1509.

Zhang, X., J. H. Helsdon Jr., and R. D. Farley (2003a), Numerical modeling of lightning-produced $NO_x$ using an explicit lightning scheme: 2. Three-

dimensional simulation and expanded chemistry, *J. Geophys. Res.*, *108*(D18), 4580, doi:10.1029/2002JD003225.

Zhang, X., J. H. Helsdon Jr., and R. D. Farley (2003b), Numerical modeling of lightning-produced $NO_x$ using an explicit lightning scheme: 1. Two-dimensional simulation as a ''proof of concept'', *J. Geophys. Res.*, *108*(D18), 4579, doi:10.1029/2002JD003224.

Ziemke, J. R., S. Chandra, B. N. Duncan, L. Froidevaux, P. K. Bhartia, P. F. Levelt, and J. W. Waters (2006), Tropospheric ozone determine from Aura OMI and MLS: Evaluation of measurements and comparison with the Global Modeling Initiative's chemistry transport model, *J. Geophys. Res.*, *111*(D19), D19303, doi:10.1029/2006JD007089.

D. Allen, Department of Atmospheric and Oceanic Science, University of Maryland, College Park, MD 20742, USA.

A. DeCaria, Department of Earth Sciences, Millersville University, P.O. Box 1002, Millersville, PA 17551-0302, USA.

S. Lang and W.-K. Tao, Mesoscale Atmospheric Processes Branch, Code 613.1, NASA Goddard Space Flight Center, Greenbelt, MD 20771, USA.

R.-F. Lin and L. Ott, Global Modeling and Assimilation Office, Code 610.1, NASA Goddard Space Flight Center, Greenbelt, MD 20771, USA. (lesley.e.ott@nasa.gov)

K. Pickering, Code 613.3, NASA Goddard Space Flight Center, Greenbelt, MD 20771, USA.

B. Ridley, Atmospheric Chemistry Division, National Center for Atmospheric Research, 1850 Table Mesa Dr., Boulder, CO 80305, USA.

G. Stenchikov, 4700 King Abdullah, University of Science and Technology, Thuwal 23995-6900, Saudi Arabia.